

**PALACKY UNIVERSITY OLOMOUC**  
**Faculty of Medicine**  
**&**  
**INSTITUTE OF MOLECULAR AND TRANSLATIONAL MEDICINE**  
**Laboratory of Experimental Medicine**



**Study of growth kinetics of 3D cultures of  
cancer cells and its effect on drug response**

**Master Thesis**

**Bc. Marta Zbožínková**

Study program: Biology

Field of study: Experimental Biology

Form of Study: Full-time

**Olomouc 2015**

**Supervisor: Mgr. Viswanath Das, PhD.**

„I declare that this Master Thesis was developed independently, under the guidance of  
Mgr. Viswanath Das, Ph.D., and using the cited literature.“

In Olomouc , .....

Signature.....

## **ACKNOWLEDGEMENTS**

This master thesis was performed at Laboratory of Experimental Medicine, Institute of Molecular and Translational Medicine in Olomouc, in collaboration with the Palacky University in Olomouc in the period October 2013 to May 2015.

Foremost, I would like to thank my supervisor Mgr. Viswanath Das, Ph.D., who has supported me throughout my thesis with his patience and friendly attitude. I greatly appreciate the knowledge that you gave me, the skills that you taught me, your time that you spent with me and, above all, the confidence that you had in me. Without you this thesis would never have been completed. One could hardly wish for a better supervisor.

Thank you Mgr. Lakshman Varanasi, Ph.D. for your precious time, advices and assistance in resolving problems associated with Western blotting. I would also like to express my gratitude to Renata Buriánová and Mgr. Petr Konečný of the Laboratory of Cell Biology, and Mgr. Anna Janošťáková and others of the Laboratory of Tissue Culture for their willingness to help.

Thank MUDr. Petr Džubák, Ph.D. for letting me use the facilities of the screening laboratory. I would like to take this opportunity to also thank Doc. MUDr. Marián Hajdúch, Ph.D., the Director of the Institute of Molecular and Translational Medicine for permitting me take this topic.

## **BIBLIOGRAPHICAL IDENTIFICATION**

Author's name	Bc. Marta Zbožíková
Title	Study of growth kinetics of 3D cultures of cancer cells and its effect on drug response
Type of thesis	Master thesis
Department	Faculty of Medicine, Palacky University & Laboratory of Experimental Medicine, Institute of Molecular and Translational Medicine
Supervisor	Mgr. Viswanath Das, Ph.D.
Year of defense	2015

### Summary

Colorectal cancer is third most common cancer not only in the Czech Republic, but also in the world. Despite the availability of standard treatment, tumor relapse and drug resistance are major clinical challenges. Effective selection of anticancer drugs in preclinical stages of drug discovery requires suitable *in vitro* cell models that mimic the *in vivo* tumor conditions. The current basic laboratory techniques of culture of cancer cells in the two-dimension do not adequately reproduce these *in vivo* tumor conditions. However, the use of three-dimensional cultures of cancer cells is becoming a highly appropriate and affordable system for effective screening of anticancer drugs under physiologically-relevant tumor conditions. This thesis focuses on the development of culture conditions for three-dimensional cultures of colorectal cancer cells as multicellular tumor spheroids for anticancer drug screening.

Keywords	3D culture, MCTSs, anticancer drugs, growth, colorectal carcinoma
Number of pages	64
Number of appendices	3
Language	English

# CONTENT

ACKNOWLEDGEMENTS .....	3
BIBLIOGRAPHICAL IDENTIFICATION .....	4
CONTENT .....	5
ABBREVIATIONS .....	7
1. INTRODUCTION .....	9
1.1 Global cancer statistics.....	9
1.1.1 CRC in the Czech Republic .....	10
1.2 Molecular basis of CRC .....	11
1.2.1 Diagnosis of CRC .....	12
1.2.2 Current treatments for CRC.....	13
1.2.3 Targeted therapy .....	13
1.3 Drug resistance mechanisms in solid tumors.....	14
1.3.1 Low penetration of drugs inside solid tumor .....	14
1.3.2 Hypoxia-induced alteration in cell proliferation.....	15
1.3.3 Tumor acidity.....	15
1.3.4 Expression of resistance-associated proteins .....	16
1.4 Three-dimensional cell culture in cancer research.....	16
1.4.1 Differences between 2D and 3D culture on the extrinsic level .....	17
1.4.2 Differences between 2D and 3D culture on the intrinsic level.....	18
1.5 Aim of the thesis .....	20
2. MATERIALS AND METHODS.....	21
2.1 Two-dimensional cell cultures .....	21
2.2 Three-dimensional MCTS cell culture.....	21

2.3	Drugs .....	22
2.4	Cell harvesting and lysis .....	22
2.5	Gel electrophoresis and Western blotting .....	23
2.6	MTT cytotoxicity Assay .....	24
2.7	MCTS growth study .....	25
2.8	ViCell viability assay .....	25
2.9	Flow cytometry .....	26
3.	RESULT 1 - Study of growth kinetics of MCTS .....	27
3.1	MCTS volume change with time .....	27
3.2	Change in viability and cell number in MCTS with time .....	31
3.3	Cell cycle changes in 3D cultures over time .....	36
3.4	Changes in the expression of CAIX and HIF-1 $\alpha$ in 3D culture .....	38
3.5	Discussion .....	39
4.	RESULT 2 .....	40
4.1	MTT Assay.....	40
4.2	Cell cycle changes in 2D and 3D culture using treatment .....	43
4.3	Changes in the expression of N-myc, caspase 8 and CAIX in 2D and 3D cultures .....	46
4.4	Discussion .....	48
5.	CONCLUSION.....	49
	REFERENCES .....	50
	APPENDIX I .....	56
	APPENDIX II.....	59
	APPENDIX III.....	61

## **ABBREVIATIONS**

ABC	ATP-binding cassette
AKT	V-Akt murine thymoma viral oncogene homolog
ALDH1	Aldehyde dehydrogenase 1
APC	Adenomatous polyposis coli
ASR	Age-standardized rate
BCA	Bicinchonic acid
BSA	Bovine serum albumin
CRC	Colorectal cancer
EGFR	Epidermal growth factor receptor
FAP	Familial adenomatous polyposis
FCS	Fetal calf serum
FOBT	Fecal occults blood test
HNPCC	Hereditary non-polyposis colon cancer
IARC	The International Agency for Research on Cancer
IC <sub>50</sub>	Half maximal inhibitory concentration
IFP	Interstitial fluid pressure
K-ras	Kirsten rat sarcoma viral oncogene homolog
MAPK	Mitogen-activated protein kinase
MCTSs	Multicellular tumor spheroids
MDR	Multidrug resistance
MTT	3-[4,5-dimethylthiazol-2-yl]-2,5-diphenyl tetrazolium bromide

P-gp	P-glycoprotein
RT	Room temperature
SMAD	Mothers against decapentaplegic homolog
TNM	Tumor Nodes Metastasis
TRIS	Tris(hydroxymethyl)aminomethan
VEGF-A	Vascular endothelial growth factor A
Wnt	Wingless-int1 homolog



# 1. INTRODUCTION

## 1.1 Global cancer statistics

Cancer is a major health risk that affects people of all age worldwide (Jemal et al., 2011). Colorectal cancer (CRC) is the third most common cancer and the fourth most common cause of death (Hagggar et al., 2009) (Table 1). The International Agency for Research on Cancer (IARC) reported 14.1 million cases of cancer with an approximate 8.2 million cancer deaths worldwide in 2012 compared to 12.7 million cancer cases and 7.6 million deaths in 2008 (Jemal et al., 2011).

*Table 1. Incidence, mortality and 5-years prevalence of various cancers among both the sexes globally (Source: IARC, Globocan 2012). ASR indicates age-standardized rate.*

	Incidence		Mortality		5-years prevalence	
	Number	ASR	Number	ASR	Number	ASR
<b>Breast</b>	1 676 633	43.3	521 817	12.9	6 255 391	19.2
<b>Prostate</b>	1 111 689	31.3	307 471	7.8	3 923 668	12.1
<b>Lung</b>	1 824 701	23.1	1 589 800	19.7	1 893 078	5.8
<b>Colorectum</b>	1 360 602	17.2	693 881	8.4	3 543 582	10.9
<b>Cervix uteri</b>	527 624	14.0	265 653	6.8	1 547 161	4.8
<b>Stomach</b>	951 594	12.1	723 027	8.9	1 538 127	4.7
<b>Liver</b>	782 451	10.1	745 517	9.5	633 170	1.9
<b>Corpus uteri</b>	319 605	8.3	76 155	1.8	1 216 504	3.7
<b>Ovary</b>	238 719	6.1	151 905	3.8	586 624	1.8
<b>Oesophagus</b>	455 784	5.9	400 156	5.0	464 063	1.4

There is a large geographic difference in the global distribution of CRC (Figure 1). Countries with the highest incidence rates of CRC include Australia, New Zealand, Canada and the U.S.A., in addition to many parts of Europe. In addition to environmental factors that contribute to CRC, other risk factors of CRC include

unhealthy dietary practices, cigarette smoking, heavy alcohol consumption, physical inactivity and obesity. The most of these factors are not typical for the countries with the lowest risk of creation colorectal carcinoma, including China, India, and parts of Africa and South America (Hagggar et al., 2009).

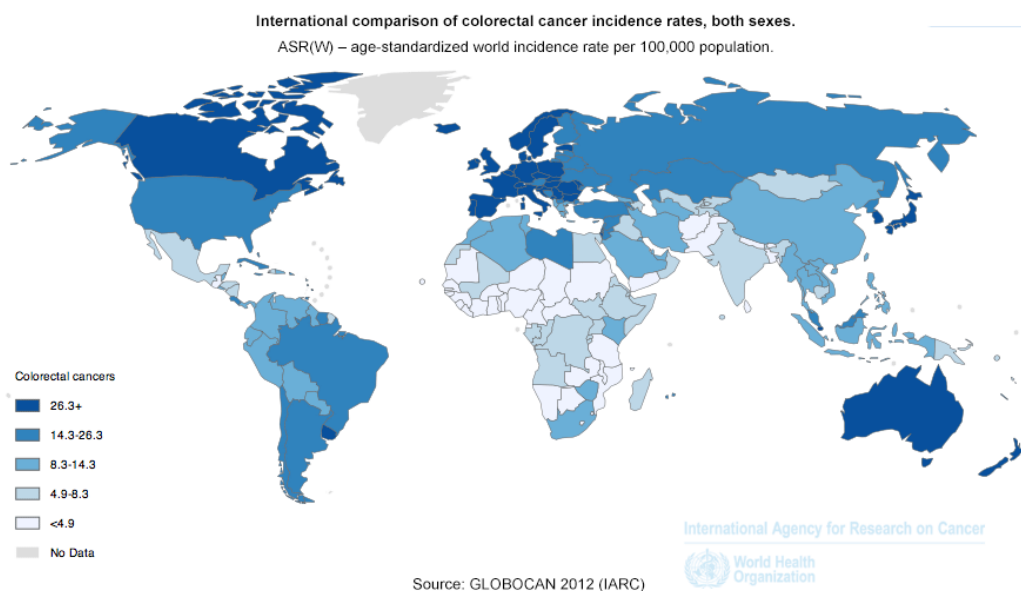


Figure 1: Global distribution of CRC incidences in both the sexes (Source: Globocan 2012). Dark blue indicates the highest incidence, light blue the lower incidence.

### 1.1.1 CRC in the Czech Republic

According to the Czech National Cancer Registry, CRC is the third most common cancer in the Czech Republic with 79 in 100 000 people affected every year ([www.svod.cz](http://www.svod.cz)). Globally, Czech Republic has the fifth highest incidence of CRC with more number of cases in men than women. In both the sexes, the prevalence of CRC increases from 40 years of age with significant increase seen around 70-75 years. In the last 5 years, however, there has been significant decrease in CRC occurrence and a record low mortality due to CRC in the Czech Republic possibly due to availability of improved diagnostic and therapeutic strategies (Figure 2).

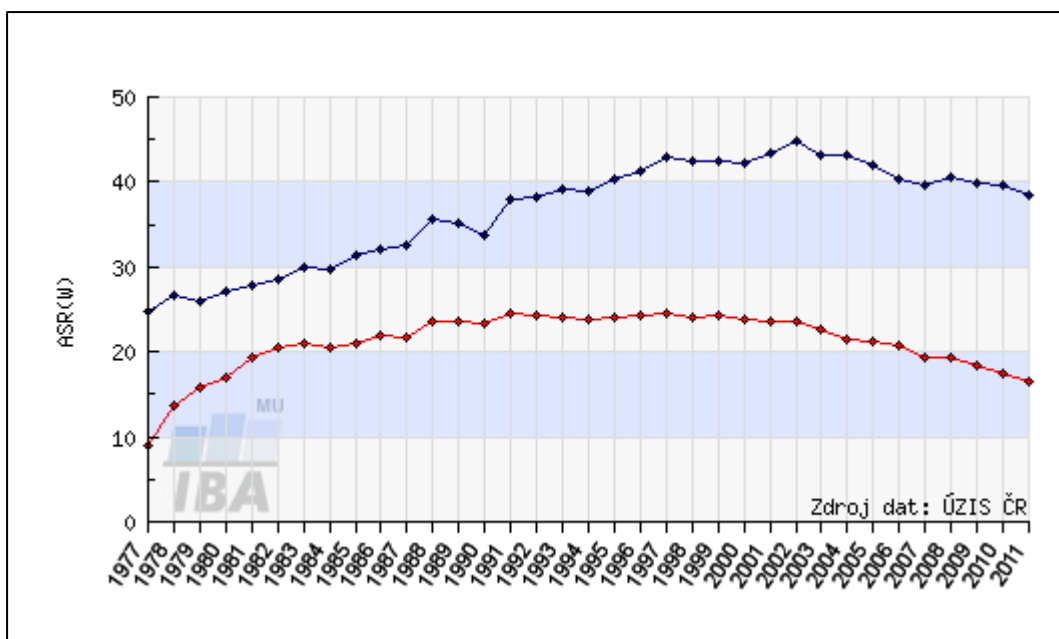


Figure 2: Trends in incidence (blue) and mortality (red) of CRC in the Czech Republic. (Source: Czech National Cancer Registry).

## 1.2 Molecular basis of CRC

Similarly to other solid tumors, CRC is a progressive and multistep disease. Apart from environmental factors, genetic factors also contribute significantly to the development of CRC. In fact, about 15% of patients can find origin of the disease in the family (Arnold et al., 2005). There are two inherited syndromes associated with the development of CRC- the familial adenomatous polyposis (FAP) and hereditary non-polyposis colon cancer (HNPCC), also known as the Lynch syndrome.

While hereditary type of CRC is caused by mutations in genes and excessive incidence of polyps, multistep processes cause sporadic CRC (Tsang et al., 2014). Carcinogenesis of CRC starts with the mutation of adenomatous polyposis coli (APC) gene in the epithelial tissue. APC protein activates  $\beta$ -catenin by phosphorylation, which result in the arrest of cell proliferation and induction of apoptosis.  $\beta$ -catenin is normally ubiquitinated and degraded in proteasomes, however, mutation in APC results in inhibition of proteasome-mediated degradation of  $\beta$ -catenin. This results in an increase in  $\beta$ -catenin in cell nucleus and hyperproliferation of epithelial tissue (Arnold et al., 2005). Additionally, alterations in *K-ras* oncogene and mutations in tumor suppressor

genes, such as *p53* and *SMAD4* also contribute to the development of neoplasia, which subsequently lead to carcinoma (Figure 3) (Markowitz & Bertagnoli, 2009).

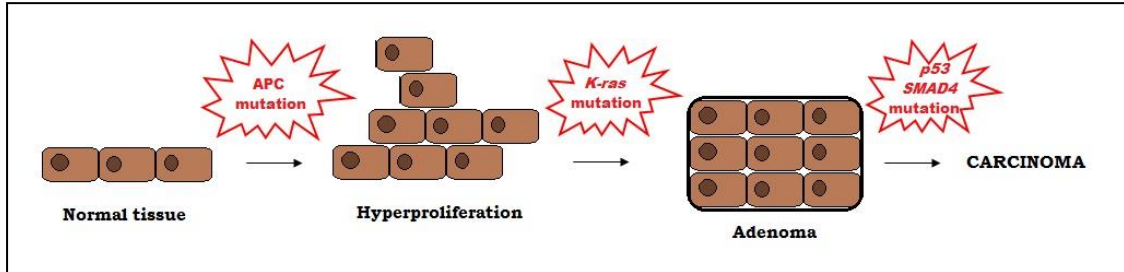


Figure 3: Carcinogenesis in CRC. Modified from Tsang et al., 2014.

### 1.2.1 Diagnosis of CRC

Due to improved screening techniques, detection of CRC is relatively simple now. There are two available strategies: fecal occult blood test (FOBT) and endoscopy. FOBT allows the detection of the most widely studied markers, carcinoembryonic antigen and CA19-9. Although due to low sensitivity and specificity of these markers, FOBT can potentially result in unreliable outcomes (Delcò & Sonnenberg, 1999). Studies have, however, indicated that if carried out under controlled conditions, FOBT can significantly reduce mortality due to CRC (Lowenfels, 2002). Compared to FOBT, the endoscopy is a more reliable in the diagnostic technique. Using sigmoidoscope or colonoscope, lesions and polyps are searched. Colonoscopy is used for most patients, and sigmoidoscopy is used in cases where anatomical reasons do not allow examination by colonoscope. According to endoscopy and biopsy results, TNM classification is done to classify the stage of tumors (Labianca et al., 2010). TNM classification of malignant tumors, also known as American Joint Committee on Cancer (AJCC) categorizes tumors stage according to a cancer staging notation system, where T (tumor) indicates invasion of primary tumor into surroundings tissues, N (nodes) indicates spread to regional lymph nodes, and M (metastasis) describes spread to other organs (O'Connell et al., 2004).

### 1.2.2 Current treatments for CRC

Standard surgery resection of tumor is the only therapy required for early-stage CRC. However, the possibility of cure by resection decreases with advance in tumor stage (Nelson et al., 2001). Often surgery resection is accompanied by a preoperative and/or postoperative radiotherapy. Studies now suggest that radiation therapy may be more effective in the treatment of CRC when combined with chemotherapy (Sauer et al., 2004). The most frequently used chemotherapeutics for CRC that have shown promising results in the clinic are 5-fluorouracil, oxaliplatin, leucovorin and irinotecan (André et al., 2004; Dietvorst & Eskens, 2013). It was found that combinations of these drugs have greater effect than using either drug alone (Goldberg et al., 2004). A number of combined formulations of these drugs are currently used clinically for CRC treatment and have shown positive results. Some of these formulations are (1) FOLFOX, consisting of 5-fluorouracil, leucovorin and oxaliplatin (Shi et al., 2012), (2) CapeOx, which is a combination of capecitabine (a derivate of 5-fluorouracil) and oxaliplatin, and (3) 5-fluorouracil in combination with leucovorin (Hirsch & Zafar, 2011; Yokomizo et al., 2013).

### 1.2.3 Targeted therapy

Survival of tumor cells depends on the activation of signaling pathways that allow uncontrolled cell proliferation and prevent apoptosis. These signaling pathways are activated by several factors, including mutations in genes and altered expression of genes and proteins. Current targeted clinical modalities approved for the treatment of CRC include bevacizumab (Avastin®), ziv-aflibercept (Zaltrap®), cetuximab (Erbix®), panitumumab (Vectibix®), and regorafenib (Stivarga®). Bevacizumab and ziv-aflibercept are monoclonal antibodies directed against vascular endothelial growth factor (VEGF) highly expressed in solid tumors. These anti-VEGF antibodies block binding of VEG to its extracellular domain and results in the inactivation of intracellular pathways for initiation of angiogenesis. The target of cetuximab and panitumumab is the epidermal growth factor receptor (EGFR) highly expressed on cancer cell surface. This factor is responsible for cell proliferation, survival, invasion and migration. Cetuximab and panitumumab prevent EGFR dimerization through steric inhibition of

the extracellular domain of EGFR (Zouhairi et al., 2011). Regorafenib is a kinase inhibitor that prevents kinase-mediated signaling pathways involved in cancer cell proliferation and tumor angiogenesis (Schmieder et al., 2014).

### **1.3 Drug resistance mechanisms in solid tumors**

Despite the availability of a number of anticancer drugs, multidrug resistance (MDR) and low cytotoxicity of anticancer drugs in solid tumors are major clinical problems. Solid tumors, like CRC have multi-level barriers that protect cancer cells from drug-induced apoptosis. Extrinsic barriers include abnormal blood vessels, hypoxia, altered cell proliferation and tumor acidity. Intrinsic barriers arise due to MDR, resulting due to mutations, genes amplifications, epigenetics modifications, alternative splicing of specific genes, etc. (Lu & Chao, 2012). These mechanisms influence drug absorption and metabolism, and the export of drugs from the cells to the extracellular space.

Tumors have a heterogeneous microenvironment made up of gradients of cells at different stages of the cell cycle, regions of hypoxia and acidity, and a necrotic core. These factors affect tumor cell response to anticancer drugs (Das et al., 2015). Monolayer cultures of cancer cells are more sensitive to certain anticancer drugs, but in clinical practice are resistant when cells grow as tumors (Hickman et al., 2014). Additionally, the extracellular microenvironment of tumors consists of not only cancer cells but also stromal cells (fibroblasts and inflammatory cells). These stromal cells secrete growth factors, chemokines and adhesion molecules, which also contribute to resistance of cancer cells to anticancer drugs (Trédan et al., 2007; Straussman et al., 2012).

#### **1.3.1 Low penetration of drugs inside solid tumor**

Another factor that contributes significantly to tumor relapse is low penetration of cytotoxic drugs inside tumors. Anticancer drugs spread to tumors by bloodstream. Although tumors create their own vasculature for growth, the walls of these vessels have fenestrations, lack basement membrane, and contain fewer pericytes than normal

tissue. These alterations result in deterioration of blood flow and decrease the delivery of drugs to the tumor (Trédan et al., 2007). Another barrier to penetration of drugs comes from increased interstitial fluid pressure (IFP) in the tumor interstitial space due to decrease in vascular permeability. Increased IFP in tumor tissue reduces transcapillary pressure gradient from vessels to interstitium, and hinders the delivery of drugs from capillaries to interstitial space (Dong & Muper, 2010). To overcome multiple drug penetration barriers and reach a lethal concentration inside cancer cells present in tumor interior, it is necessary to use sufficient concentration of anticancer drugs (Cowan & Tannock, 2001; Tannock et al., 2002).

### 1.3.2 Hypoxia-induced alteration in cell proliferation

Nutrients and oxygen are supplied to tumor cells via blood vessels and tumor cells that reside around these blood vessels receive their adequate supply. Increase in the distance from blood vessels result in induction of hypoxia due to limited supply of oxygen and nutrients. One of the main effects of hypoxia is the arrest of cells in the G<sub>1</sub> phase of the cell cycle. Anticancer agents that are effective against cells in proliferation phase fail to induce cytotoxicity in quiescent cells, resulting in survival of cancer cells in the tumor interior (Trédan et al., 2007).

### 1.3.3 Tumor acidity

The pH in microenvironment of tumor can affect the cytotoxicity of some chemotherapeutics. The pH in extracellular space is low, whereas pH of intracellular space is neutral or weakly alkaline in cancer cells. Drugs diffuse passively in neutral form; however, if drugs have an acidic dissociation constant and are protonated, the possibility of diffusion is decreased. Alkalization of the extracellular space supports the absorption of some of these drugs, on the contrary, acidic microenvironment inhibit uptake of some drugs (Gerweck et al., 2006).

#### 1.3.4 Expression of resistance-associated proteins

MDR is an intrinsic or acquired ability of cancer cells to resist multiple drugs by mechanisms such as increased efflux of drugs, activation of detoxifying systems, activation of DNA repair mechanisms or protection from induced apoptosis (Gillet & Gottesman, 2010). The efflux of drugs is mediated by ATP-binding cassette (ABC) transporters, which are usually overexpressed in tumors. It is a transmembrane protein that utilizes the energy generated from the hydrolysis of ATP to pump toxins out of cells. The best-known ABC transporter is the P-glycoprotein (P-gp) that effluxes anticancer drugs such as paclitaxel or doxorubicin (Dong & Muper, 2010). Detoxification is induced by overexpression of detoxifying enzymes, for example ALDH1 in many solid tumors (Vinogradov & Wei, 2012). Cancer cells also develop survival strategies against drug-induced apoptosis by activation signaling pathways (Aoudjit & Vuori, 2012). The Wnt proteins of Wnt signaling pathway serve as growth factors for cell proliferation in normal cells; however, in cancer cells, activated Wnt signaling enhances drug resistance by increased  $\beta$ -catenin expression (Vinogradov & Wei, 2012). Likewise, a normal Notch signaling maintains a normal level of cell proliferation and apoptosis in cells. In cancer cells, Notch ligand is strongly bound to its receptor, which leads to continuous cleavage of the intracellular domain. This domain continues to the nucleus, where it binds to transcription factors and maintains proliferation (Lobry et al., 2011).

#### 1.4 Three-dimensional cell culture in cancer research

The use of *in vitro* cell culture models that closely recapitulate *in vivo* tumor conditions is becoming an important tool for screening of anticancer drugs. Monolayer cultures of cancer cells in the two-dimension are conventional culture tools widely used in preclinical drug research. Unfortunately, two-dimensional (2D) cultures of cancer cells do not entirely recapitulate *in vivo* conditions of solid tumors. Interestingly, three-dimensional (3D) cultures of cancer cells closely reproduce *in vivo* tumor conditions are becoming an important research tool in drug discovery (Breslin & O'Driscoll, 2013).



#### 1.4.1 Differences between 2D and 3D culture on the extrinsic level

One of the major differences between 2D and 3D cultures of cells is seen in individual cell morphology. In 2D cultures, cells grow as homogenous layer; while cells are arranged as heterogeneous spatial clusters in 3D cultures. Cells cultured in 2D have a flat morphology, adhere to the substrate and spread only in the horizontal plane that result in low cell-cell contact. Flattening of cells reduces the distance between the membrane and nucleus, and cause altered cell signaling. On the contrary, cells in multicellular tumor spheroids (MCTS) have 3D morphology and spread both in horizontal and vertical planes. This allows more cell-cell contact that affects cell proliferation, apoptosis and differentiation (Baker & Cehn, 2012).

MCTS have a gradient of oxygen and nutrients from the outer to inner regions. Cells on the surface of MCTS are well-oxygenated, while those in the center are hypoxic, mimicking conditions of solid tumor (Figure 4). In contrast, cells in 2D cultures are well-oxygenated and have homogenous supply of nutrients, and thus lack the physiological gradient observed in solid tumors (Hirschhaeuser et al., 2010).

Cells in the outer layers of MCTS with good access to nutrition are proliferating, while hypoxic cells located centrally are quiescent (Wenzel et al., 2014). Majority of cells in the outer region of MCTS are in G<sub>2</sub>/M phase of the cell cycle, while hypoxic quiescent cells in the MCTS center are in early G<sub>1</sub>. Cells in 2D cultures are, however, in different phases of the cell cycle (Laurent et al., 2013).

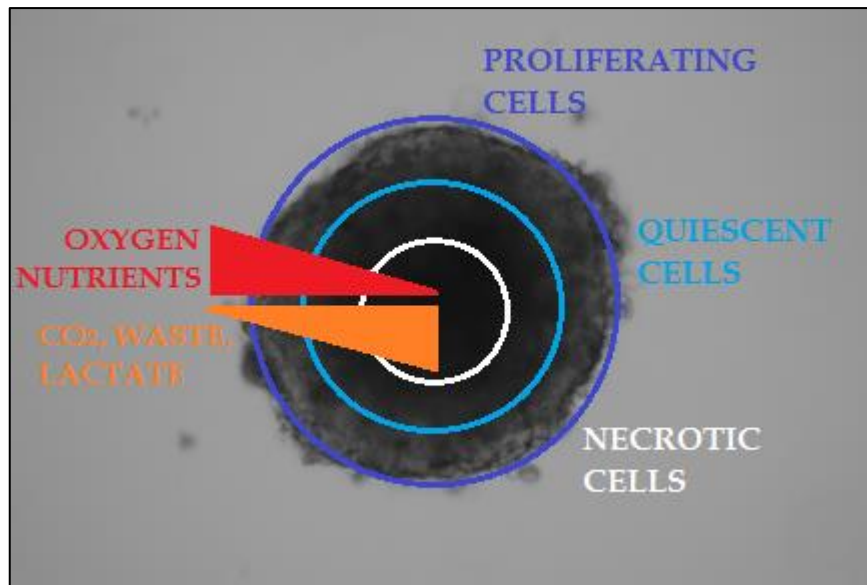


Figure 4: Characteristics of MCTS. MCTS reproduce *in vivo* tumor characteristics and display an outer layer of well-oxygenated and nourished proliferating cells in  $G_2/M$  phase of the cell cycle, inner layer of quiescent cells in  $G_1$  phase and central layer of hypoxic necrotic cells. Levels of oxygen and nutrients are high in the outer than inner regions of MCTS. Conversely, the levels of  $CO_2$ , metabolites and lactate are high in the inner than outer regions of MCTS.

Hypoxia, altered pH and multiple layers of cells in MCTS results in drug penetration barrier that complicate penetration of drug into the core of MCTS. These recapitulate multiple drug penetration barrier observed in solid tumors. Treatment of MCTS with anticancer drugs results in cell death mostly in the surface, while majority of cells in the inner regions remain unaffected. In contrast, 50% of cell's surface in 2D cultures is exposed to drugs, resulting in significant cytotoxicity compared to 3D cultures (Breslin & O'Driscoll, 2013).

#### 1.4.2 Differences between 2D and 3D culture on the intrinsic level

Mechanisms that affect the cell cycle are important for better understanding of unregulated proliferation of cancer cells. These mechanisms are dependent on cell-cell and cell-extracellular matrix interactions, and are often not present in 2D cultures (Lorenzo et al., 2011). These result in loss of many cancer-related hallmarks in 2D cell cultures that are indispensable for understanding molecular pathways of carcinogenesis.

Studies show that there is significant difference in the expression of genes and proteins in 2D and 3D cultures of cells (Table 2). Altered expression of genes effects cell signaling pathways leading to changes in cell proliferation and apoptosis following treatment with drugs (Fatima et al., 2008). Other major differences observed in cell signaling pathways in 2D and 3D cultures are seen in metabolic pathways and expression of metabolism-associated proteins (Luca et al., 2013). These proteins include transcriptional factors and serine/threonine kinases that influence metabolic pathways such as mitochondrial metabolism, glucose metabolism or glutaminolysis (Grimm et al., 2014). For example, 2D cultures of CRC cells show increased phosphorylation of Akt and MEK1/2, while 3D cultures have increased phosphorylated MAPK and decreased EGFR versus control. Gene expression of JunD and Bcl6 was also increased in 3D cultures, whereas c-Myc was decreased (Luca et al., 2013).

*Table 2: Differences in the expression of various genes in 2D and 3D cultures. ↑ indicates an increase versus control; ↓ indicates a decrease versus control. Modified from Luca et al., 2013.*

	<b>2D cultures</b>	<b>3D cultures</b>	<b>Influenced signaling pathway</b>
<b>Akt</b>	↑	↓	Akt/PKB
<b>β-catenin</b>	No difference	No difference	Wnt
<b>Bcl6</b>	↓	↑	transcription
<b>c-Myc</b>	↑	↓	apoptosis
<b>EGFR</b>	↑	↓	Akt, MAPK, JNK
<b>JunD</b>	↓	↑	apoptosis
<b>Phosphorylated MAPK</b>	↑	↑	MAPK
<b>Total MAPK</b>	↓	↑	MAPK
<b>MEK1/2</b>	↑	↓	MAPK

## 1.5 Aim of the thesis

The primary aim of this thesis was to study the changes occurring in MCTS of HCT116, HT29 and HeLa cell lines over time. MCTS of different size and cell types behave differently when cultured under the same growth condition. Therefore, it is important to understand these differences between MCTS of different cell lines for their potential use in screening of anticancer compounds.

Aim 1- Our first aim was to determine the most suitable conditions, such as cell seeding density, duration of MCTS culture that did not affect their growth due to nutrient deprivation, changes in hypoxia-associated proteins, etc. for culturing of MCTS of HCT116, HT29 and HeLa cell lines. To achieve this aim, our objectives were-

1. To determine the growth kinetics of MCTS of different size by determining the changes in spheroid size over 10 days in culture.
2. To determine cell viability and cell cycle changes in MCTS of different size over time.
3. To determine the changes in the expression of HIF-1 $\alpha$  and CAIX proteins.

Aim 2- Our second aim was to select the most suitable culture condition from Aim 1 to determine the potential effects of a few selected anticancer drugs on MCTS of HCT116 and HT29 cells, and compare this effect to 2D culture of the same cells. To achieve this aim, our objectives were-

1. To perform MTT cell proliferation assay on 2D and 3D cultures of cells following treatment with drugs.
2. To determine cell cycle changes on drug-treated 2D and 3D cultures.
3. To determine changes in the expression of a few selected apoptosis-related proteins in 2D and 3D cultures after drug treatment.

## 2. MATERIALS AND METHODS

### 2.1 Two-dimensional cell cultures

Three different established cancer cell lines were used in this study (Table 3). Human colorectal carcinoma HT29 and HCT116 cells were grown in McCoy's 5A medium (Sigma-Aldrich, Missouri, USA) supplemented with 1.5 mM L-glutamine (Sigma-Aldrich), 10% fetal calf serum (FCS; PAN-Biotech GmbH, Aidenbach, Germany), and 100 U/mL penicillin and 50 µg/mL streptomycin (Sigma-Aldrich) and will be referred as "enriched McCoy's medium". Human cervical carcinoma HeLa cells were cultured in Dulbecco's Modified Eagle's Medium (DMEM; Sigma-Aldrich) supplemented with 1.5 mM L-glutamine, 10% FCS, and 100 U/mL penicillin and 50 µg/mL streptomycin, and is referred as "enriched DMEM". All cells were maintained at 37°C in 5% CO<sub>2</sub> humidified incubator. Cells were passaged twice weekly and routinely checked for mycoplasma contamination.

*Table 3: Used cell lines.*

Cell line	Company	
HCT 116	Horizon	Cambridge, UK
HT-29	ATCC	Virginia, USA
HeLa	ATCC	Virginia, USA

### 2.2 Three-dimensional MCTS cell culture

Cells were thawed from frozen stocks and cultured in appropriate enriched medium for at least 3 passages before the start of MCTS culture. MCTS were formed using liquid-overlay culture method with slight modifications (Friedrich et al., 2007). Briefly, single-cell suspension of cells was seeded into 0.75% agarose-coated (Appendix I) 96-well plates and/or 384-well plates using a Multidrop™ Combi Reagent Dispenser (Thermo Fisher Scientific Inc., MA, USA). Plates with cells were incubated for 30 min at 37°C in an incubator to allow cells to settle to the bottom of the plate. Plates were centrifuged

using an Eppendorf benchtop centrifuge for 30 min, and left undisturbed for 4 days in a SteriStore rotary incubator at 37°C, with 5% CO<sub>2</sub> and 95% humidity. On the 4<sup>th</sup> day, 50% of supernatant was replaced by fresh enriched medium and MCTS were routinely monitored using a phase contrast microscope. The medium was routinely replaced every 2 days till the start of drug treatment.

## 2.3 Drugs

Standard anticancer drugs used in this study were purchased from companies as listed in Table 4. Mechanisms of action of 7 selected drugs are described in Appendix II.

*Table 4: List of anticancer agents used in this study*

Active substance	Generic name	Mechanism of action	Company, Country
<b>Cisplatin</b>	Cisplatin“Ebewe”	Alkylating agent	Ebewe Pharma, AT
<b>Doxorubicin</b>	Doxorubicin Teva	Antitumor antibiotics	Teva Pharmaceuticals, CZ
<b>Fluorouracil</b>	Fluorouracil	Antimetabolite	Hospira UK Limited, UK
<b>Gemcitabine</b>	Gemzar®	Antimetabolite	Lilly, USA
<b>Irinotecan</b>	Campto®	Plant alkaloid	Pfizer spol. s.r.o., CZ
<b>Paclitaxel</b>	Taxol®	Plant alkaloid	Bristol-Myers Squibb, USA
<b>Vincristine</b>	Vincristine Teva	Plant alkaloid	Teva Pharmaceuticals, CZ

## 2.4 Cell harvesting and lysis

Treated and/or untreated cells in monolayer were washed with 1× phosphate-buffered saline (PBS) and detached from the bottom of plates using Tryple/EDTA solution (Cat. # 12563-029, Life Technologies, CA, USA). Cells were collected into Eppendorf tubes and centrifuged at 300× g for 5 min. Supernatant was then removed, and cell pellet was resuspended in a cell lysis buffer (Appendix I). Similarly, treated and/or untreated MCTS were collected into Eppendorf tubes, washed with 1× PBS and centrifuged to remove the supernatant. MCTS were then dissociated into single-cell suspension using Accutase® Cell Detachment Solution (Cat. # A6964, Sigma-Aldrich). Dissociated cells were washed with 1× PBS and centrifuged at 300× g to remove Accutase®. Cells were

then resuspended in the cell lysis buffer as monolayer cultures, and lysed on an orbital shaker in a cold room by gently shaking the Eppendorf tubes for 45 min. Lysed cells were then centrifuged in a benchtop centrifuge (Model # 5810R, Eppendorf AG, Hamburg, Germany) at 4°C for 20 min at 13 000 rpm. The supernatant was collected into a new ice-cold Eppendorf tube, and the protein concentration was quantified using a Pierce™ BCA Protein Assay Kit (Cat. # 23225, Life Technologies) following manufacturer's protocol. The absorbance was measured using an EnSpire® Multimode Plate Reader (Model # 2300-001M, Perkin Elmer, Waltham, USA) at 562 nm. Protein samples were either used immediately or stored at -80°C for later processing.

## **2.5 Gel electrophoresis and Western blotting**

Protein samples were mixed with 5× SDS loading buffer (Appendix I), and heated for 5 min at 95°C. Fifteen µL of protein was loaded per well and electrophoresed by 10% SDS-PAGE in 1×Tris/Glycin/SDS running buffer (Cat. # 161-0732, BioRad, CA, USA) at 150 V for 90 min using standard protocols for SDS-PAGE. Four µL of Spectra™ Multicolor Protein Ladder (Cat. # 26625, Life Technologies) was loaded in a separate well and run alongside protein samples. Following electrophoresis, proteins were transferred to a low background fluorescence Immobilon FL membrane (Cat. # IPVH00010, Millipore Corp., Billerica, MA, USA) using Tris/Glycine transfer buffer (Cat. # 161-0734, BioRad). Western blot transfer was carried out at 21 V for 17 h in a cold room to avoid overheating of the transfer apparatus.

Immunoblots were blocked in a blocking buffer consisting of 5% bovine serum albumin (BSA) dissolved in 1× PBS (pH 7.5) with 0.1% Tween-20 (PBST; Appendix I) at room temperature (RT) for 2 h. Blots were incubated with primary antibodies (Table 5) for overnight at 4°C. Following an overnight incubation with primary antibodies, immunoblots were incubated with secondary antibodies (Table 5) for 2 h at RT in dark. Immunoblots were washed 3× regularly with 1× PBST following blocking and incubation with primary antibodies. After 2 h of incubation with secondary antibody, immunoblots were washed 3× with 1×PBS, and protein bands visualized using a ChemiDoc™ MP Analyzer (BioRad) using appropriate filters. For restaining of immunoblots for proteins with similar molecular weights, the membranes were stripped

for 20 min in Restore™ Stripping Buffer (Cat. # 46430, Life Technologies) at RT. Following stripping, membranes were washed 3× with deionized water, and reprobbed with remaining antibodies.

*Table 5: List of primary and secondary antibodies used in this study*

	<b>Antibody</b>		<b>Company</b>	<b>Dilution</b>	<b>Host</b>	<b>Isotype</b>	<b>Clonality</b>
<b>Primary antibodies</b>	Actin		Sigma Aldrich	1:3000	Mouse	IgG2a	Monoclonal
	CA IX		Novus Biological	1:1000	Rabbit	IgG	Polyclonal
	HIF1- $\alpha$		Novus Biological	1:1000	Rabbit	IgG	Polyclonal
	N-myc		Calbiochem	1:1000	Mouse	IgG1	Monoclonal
	Caspase 8		BD BioSciences	1:500	Rabbit	IgG2a	Polyclonal
	Pg-p		Sigma Aldrich	1:1000	Mouse	IgG1	Monoclonal
<b>Secondary antibodies</b>	Alexa	Fluor	Life Technologies	1:1000	Goat anti-	-	-
	633				Mouse		
	Alexa	Fluor	Life Technologies	1:1000	Goat anti-	-	-
	488				Rabbit		

## 2.6 MTT cytotoxicity Assay

MTT assay is a method based on reduction of 3-[4,5-dimethylthiazol-2-yl]-2,5-diphenyl tetrazolium bromide into violet formazan crystals by dehydrogenases of living cells. Addition of SDS dissolves formazan crystals and results in their release from cells.

For MTT assay on 2D cultures, cells were plated in triplicate in a 96-well at a density of  $1 \times 10^5$  cells/well in enriched medium. Drugs were added to the first set of triplicate wells, and thereafter serially diluted. Control and blank wells were also included in triplicate. Cells were treated with drugs for 72 h at 37°C in a 5% CO<sub>2</sub> humidified incubator. After 72 h, 10  $\mu$ L MTT from a 5 mg/mL stock solution (Appendix I) was added to each well, and the plates were incubated at 37°C for 4 h. After 4 h, SDS was added to each well to dissolve formazan crystals and the plates were further incubated at 37°C for overnight. The absorbance of the plate was read the next day in an EnVision Multimode Plate Reader (Perkin Elmer, Waltham, USA). The data



were analyzed as the percent of control well absorbance and the half maximal inhibitory concentration (IC<sub>50</sub>) of drugs determined by plotting a concentration-response curve using Sigma Plot software (Version 10, Systat Software, Inc., Point Richmond, CA). The IC<sub>50</sub> was calculated using the equation,  $y = \min + [\max - \min / (1 + 10^{(\log \text{IC}_{50} - X) \cdot \text{hillslope}})]$ , where  $y$  = percentage of control,  $x$  = concentration, 'max' and 'min' are the maximum and minimum measured values, respectively.

For MTT assay on MCTS, spheroids were collected into a 50 mL Falcon tube and washed 2× with 1× PBS to remove medium. Spheroids were dissociated into single-cell suspension using Accutase® at 37°C. Cell viability of the single-cell suspension solution was assessed using the ViCell® XR Cell Viability Analyzer (Beckman Coulter Inc., USA). Cells were plated in a 384-well plate at a density of 1000 cells/well using the Multidrop™ Combi Reagent Dispenser and allowed to attach to plate bottom in an incubator at 37°C for overnight. Following an overnight incubation, cells were treated with anticancer drugs for 72 h and an MTT assay performed similar to 2D cultures to determine IC<sub>50</sub> values.

## **2.7 MCTS growth study**

This experiment was performed to monitor the growth of HCT116, HT29 and HeLa cell MCTS in real-time. MCTS of different size were imaged using a 10× objective in an inverted fluorescent microscope (Carl Zeiss Axio Observer.D1). Phase contrast images of MCTS were acquired using an Axio Camera MRC5 attached to the microscope every 2 days for 5 days. Same MCTS were imaged every 2 days, and at least six MCTS were imaged per cell line per experiment. Images were stored as .czi file and MCTS diameter was calculated manually using the ZEN Pro software (Carl Zeiss), and later processed to obtain MCTS volume.

## **2.8 ViCell viability assay**

MCTS were collected every 2 days into Eppendorf tubes and dissociated into single-cell suspension using Accutase® at 37°C. Dissociated cells were washed with 1×PBS to remove Accutase® and cell viability measured using the ViCell® XR Cell Viability

Analyzer. The Analyzer is able to determine cell properties such as diameter, circularity, and cell viability following staining cell suspension with trypan blue.

## **2.9 Flow cytometry**

Cells were seeded in 6-well plates and treated with drugs for 72 h. Cells were washed with 1× PBS, detached from the bottom of wells using Tryple/EDTA solution and collected into tubes. Cells were then fixed using 70% ethanol for overnight at 4°C. Thirty equal-sized MCTS were collected, after 4 days of initiation, from 384-well plates into one well of 12-well plate and treated with anticancer agents for 72 h. Treated MCTS were dissociated into single-cell suspension and fixed with 70% ethanol at 4°C for overnight.

Tubes were removed from fridge and centrifuged at 800× g for 5 min. Ethanol was removed, fixed cells were then resuspended in citrate buffer (Appendix I) and centrifuged at 800× g for 7 min. Then, 300 μL of propidium iodide (Appendix I) was added and cells were incubated for 15 min at 37°C in the dark to stain the DNA. RNAase solution was added for 15 min at 37°C. Tubes were stored for 1 hour at 4°C and then measured using CellQuest™ Pro Software (BD BioScience) on Mac® OS9 and BD FACSCalibur Cell Analyzer (BD Biosciences, CA, USA). The data was processed using ClarisWorks (Macintosh).

### **3. RESULT 1 - Study of growth kinetics of MCTS**

#### **3.1 MCTS volume change with time**

To study the change in the volume of MCTS of different cell lines with time, we were monitored their growth every 2 days by phase contrast microscopy. MCTS of four different size were used for HCT116 and HT29, whereas, only two sizes were used for HeLa MCTS. Images were analyzed to measure the Feret's diameters using Zen Blue image analysis software. Feret's diameters were used to calculate the volume.

The large-sized MCTS ( $1 \times 10^5$  cell/mL) of both HCT116 and HT29 attain a plateau on Day 4 of culture, and MCTS of HCT116 start to shrink following 8 days in culture. In all the cell lines, MCTS of smallest size showed a steady growth over 10 days in culture. Additionally, with increase in size there is slow disintegration of MCTS as evidenced from deposition of loose cells around MCTS. HCT116 formed most compact MCTS (Figure 5), while HeLa MCTS, irrespective of size, were loosely packed (Figure 7).

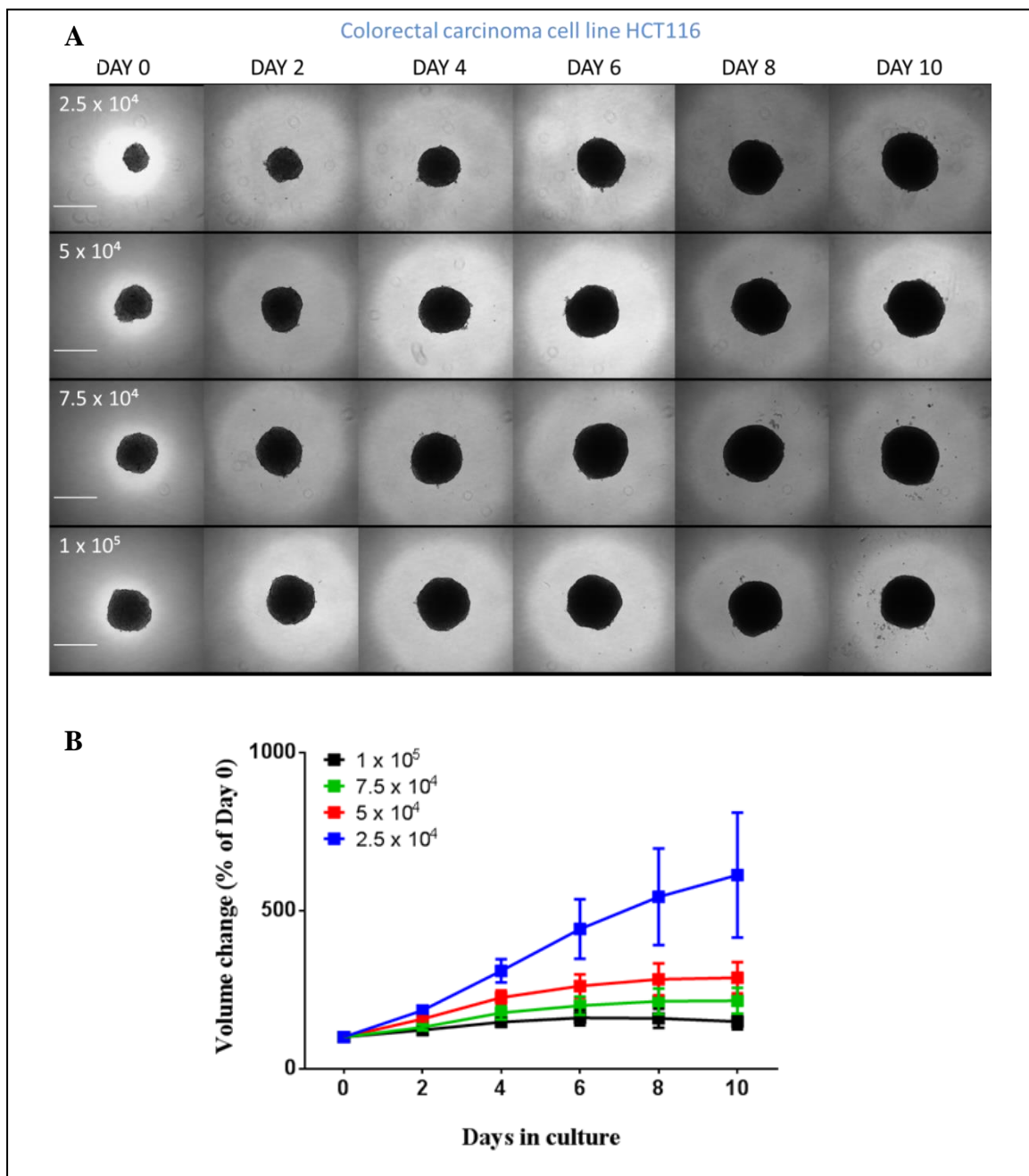


Figure 5: Growth of HCT116 cell line in 3D culture. (A) Images of HCT116 MCTS of four different sizes ( $2.5 \times 10^4$ ,  $5 \times 10^4$ ,  $7.5 \times 10^4$  and  $1 \times 10^5$  cells/mL) over 10 days in culture are shown. 10 $\times$  objective, scale bar- 500  $\mu$ m. (B) Growth curve of HCT116 MCTS is presented to show change in MCTS volume over 10 days. Volumes of MCTS on day 2-10 are normalized to their respective volume on Day 0 for each size of MCTS. Data are presented as mean  $\pm$  SD of at least 6 MCTS per size from 3 independent experiments.

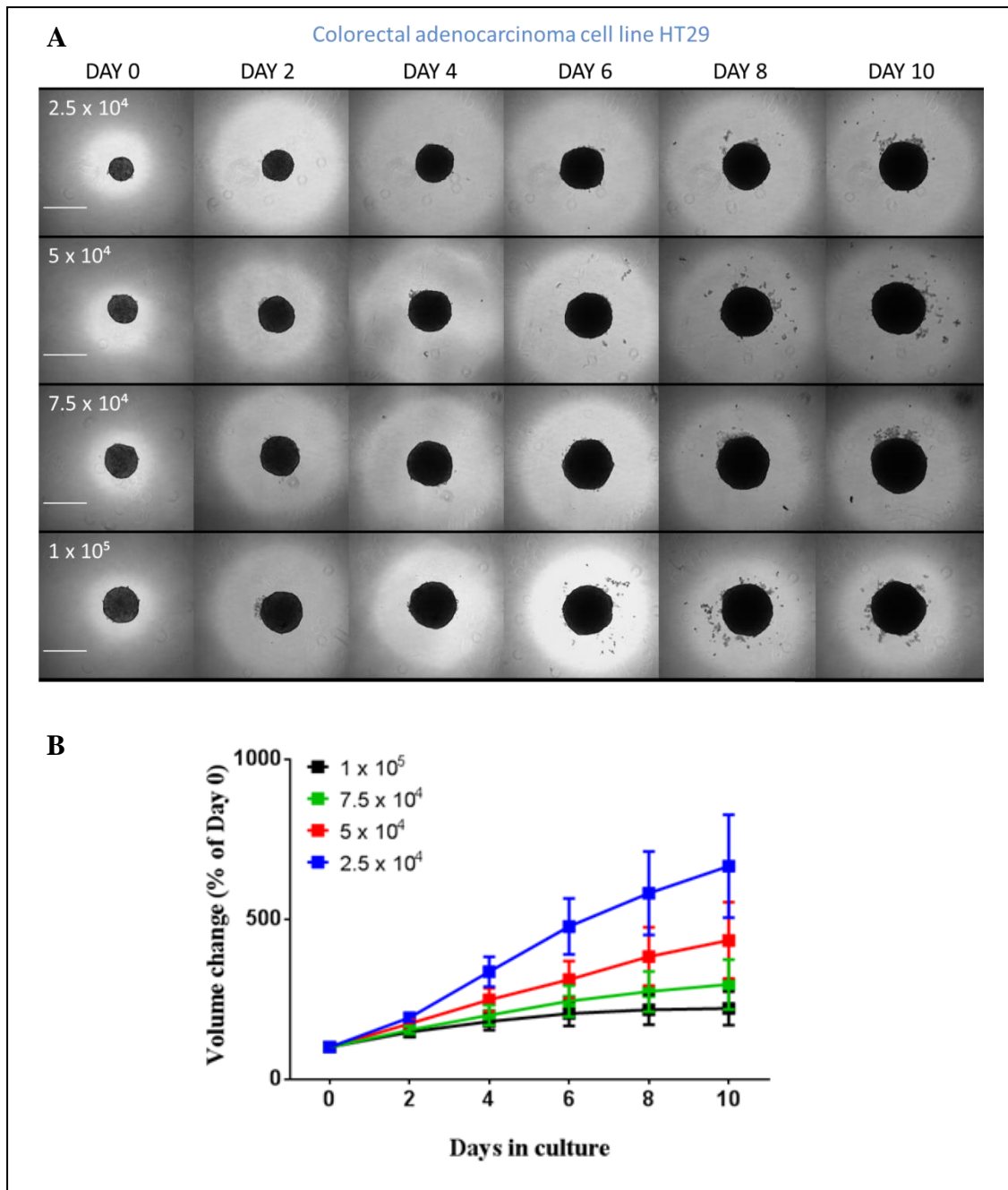


Figure 6: Growth of HT29 cell line in 3D culture. (A) Images are presented of HCT29 MCTS of four different sizes ( $2.5 \times 10^4$ ,  $5 \times 10^4$ ,  $7.5 \times 10^4$  and  $1 \times 10^5$  cells/mL) taken every 2 days over a 10-day period. 10 $\times$  objective, scale bar- 500  $\mu$ m. (B) The graphical representation of growth kinetics of HT29 MCTS over 10-day period. Data are presented as mean  $\pm$  SD of at least 6 MCTS per size from 3 independent experiments.

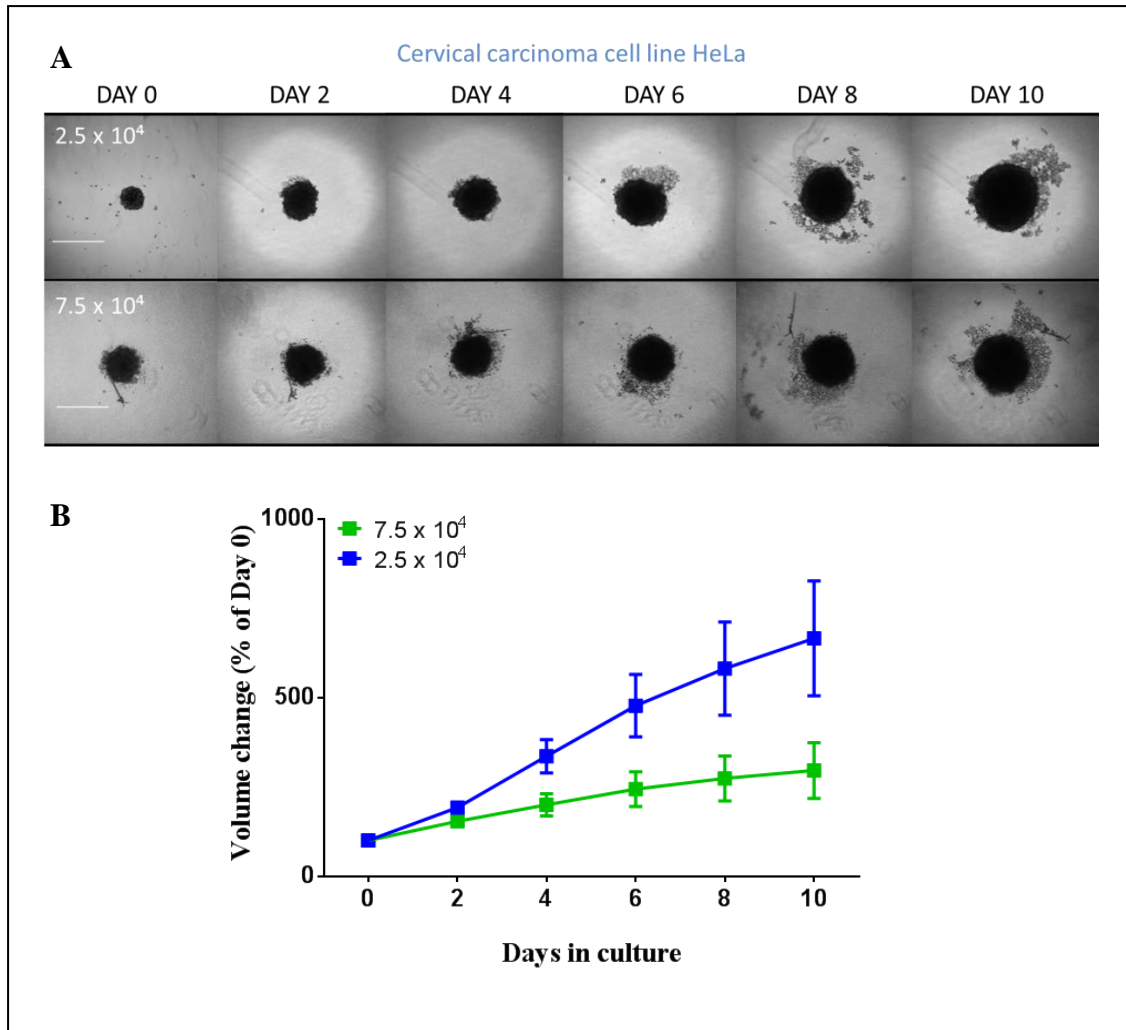


Figure 7: Growth kinetics of HeLa cell line in 3D culture. (A) Images of HeLa MCTS taken every 2 days for 10 days are presented. Compared to HCT116 and HT29 MCTS, HeLa cells formed loose MCTS that start to disintegrate from Day 6. Only two MCTS size was chosen for HeLa cells. 10 $\times$  objective, scale bar- 500  $\mu$ m. (B) A graph is presented to show change in volume of MCTS relative to Day 0. Data are presented as mean  $\pm$  SD of at least 6 MCTS per size from 3 independent experiments.

### 3.2 Change in viability and cell number in MCTS with time

To determine 3D microenvironment-induced changes on cell viability, total cell number, and single-cell diameter, MCTS were collected every 2 days and analyzed by Cell Analyzer. Four sizes were used for HCT116 and HT29 cell MCTS (sizes-  $2.5 \times 10^4$ ,  $5 \times 10^4$ ,  $7.5 \times 10^4$  and  $1 \times 10^5$  cell/mL), and only two sizes for HeLa MCTS (sizes-  $2.5 \times 10^4$  and  $7.5 \times 10^4$  cell/mL).

#### *1 × 10<sup>5</sup> cell/mL MCTS of HCT116 and HT29*

Viability of cells in the MCTS of size  $1 \times 10^5$  cell/mL of both HCT116 and HT29 decreased slightly from day 6 to day 10. Total cell number increases in HT29, while number of total cells of HCT116 slightly decreased in size  $1 \times 10^5$ . There is no major change in the single-cell diameter in MCTS of both the cell lines (Figure 8).

#### *7.5 × 10<sup>4</sup> cell/mL MCTS of HCT116, HT29 and HeLa*

Cell viability decreases from day 6 to day 10 in HCT116, HT29 and HeLa MCTS of size  $7.5 \times 10^4$ . There is an increase in the total cell number in HT29 and HeLa MCTS increase. However in HCT116 MCTS, there is no increase in total cell number rather a decrease in total number of cells from day 8. The diameter of single cells in MCTS slightly decreases in both colorectal cancer cell lines, while slightly increases in HeLa cell line (Figure 9).

#### *5 × 10<sup>4</sup> cells/mL MCTS of HCT116 and HT29*

Similar to previous two sizes, the viability of both HCT116 and HT29 MCTS decreases from day 6. Total cell number in HT29 MCTS increases from day 6, while total cell number of in HCT116 MCTS decreases from day 8. The diameter slightly decreases from day 6 in both cell lines (Figure 10).

#### *2.5 × 10<sup>4</sup> cells/mL MCTS of HCT116, HT29 and HeLa*

The viability of cells in MCTS of all cell lines decreases from day 6 in the smallest MCTS, however, the viability of HCT116 and HT29 continues to fluctuate, while viability of HeLa cell line continues to decrease. The total cell number of all cell

lines increases, whereas diameter slightly decreases in HCT116 and HT29 cells from day 6 and slightly increases in HeLa cell line (Figure 11).

In general, the viability of cells of all sizes in all cell lines decreased from day 6. While the total cell number is showed alteration in relation to cell line and size of MCTS. However, the total cell number significantly increases in the smallest MCTS with  $2.5 \times 10^4$  cells/mL cell seeding density on day 8 and 10 compared to other sizes.

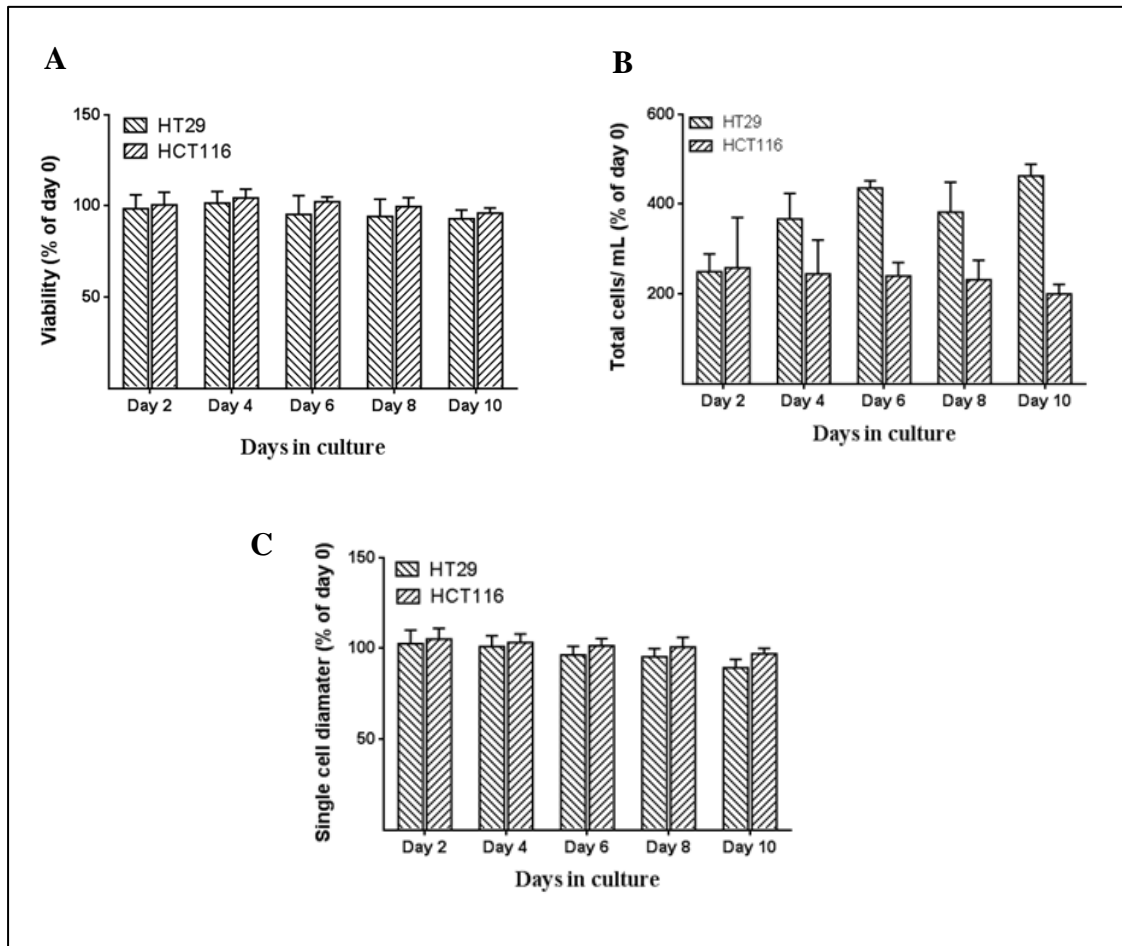


Figure 8: Effect of growth on (A) viability, (B) total cell number and (C) single-cell diameter of MCTS of size  $1 \times 10^5$  cell/mL in HCT116 and HT29. Data are the mean  $\pm$  SEM,  $n = 3$ .



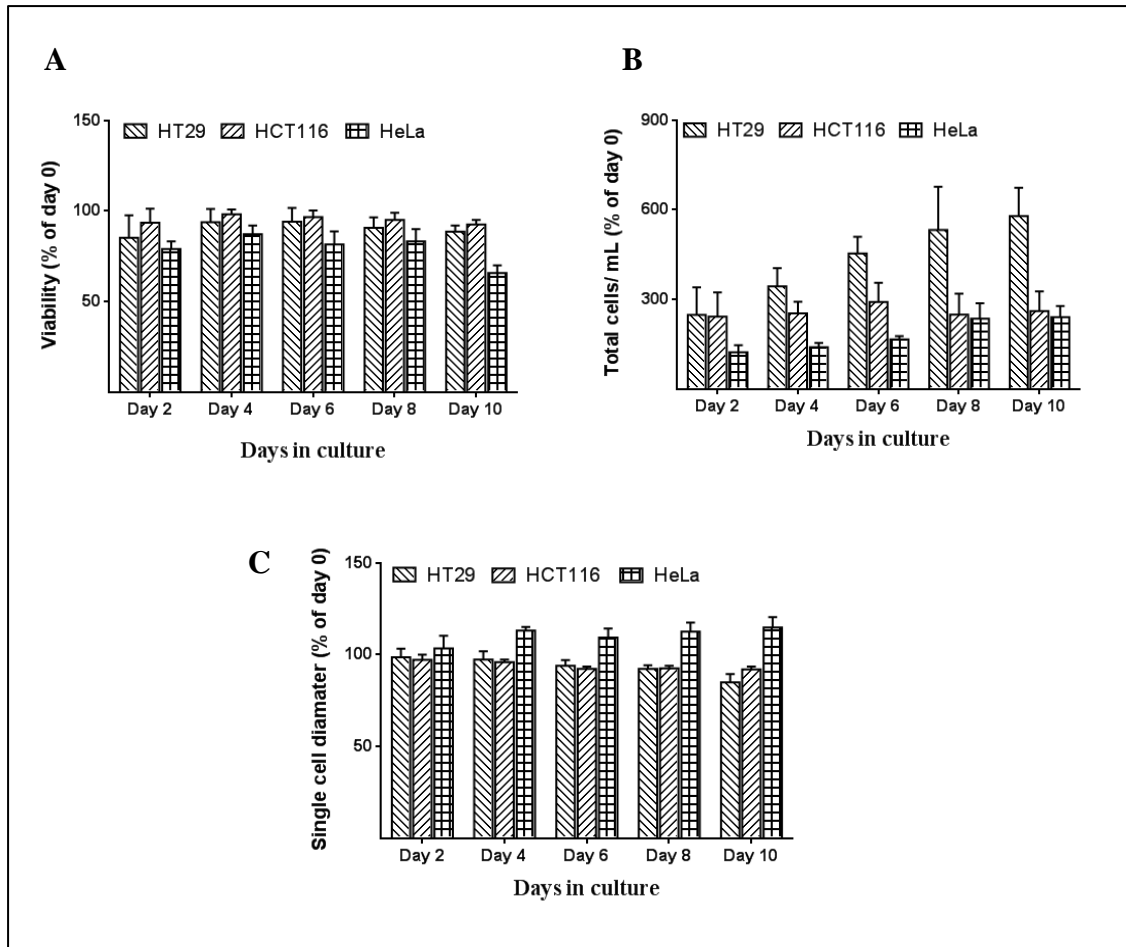


Figure 9: Effect of growth on (A) viability, (B) total cell number and (C) single-cell diameter of MCTS of size  $7.5 \times 10^4$  cell/mL in HCT116, HT29 and HeLa. Data are the mean  $\pm$  SEM,  $n = 3$ .

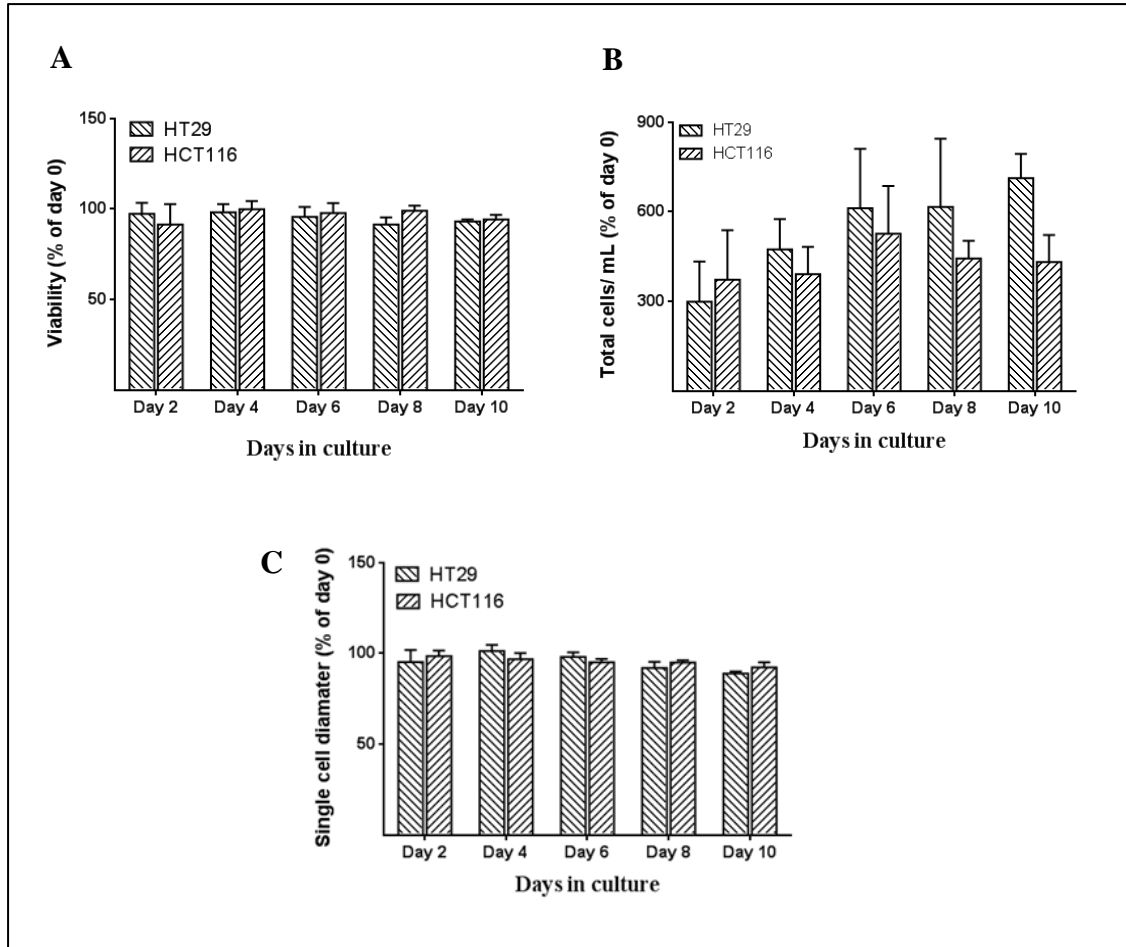


Figure 10: Changes in the (A) viability, (B) total cell number and (C) single-cell diameter in HCT116 and HT29 MCTS of size  $5 \times 10^4$  cell/mL with culture time. Data are the mean  $\pm$  SEM,  $n = 3$ .

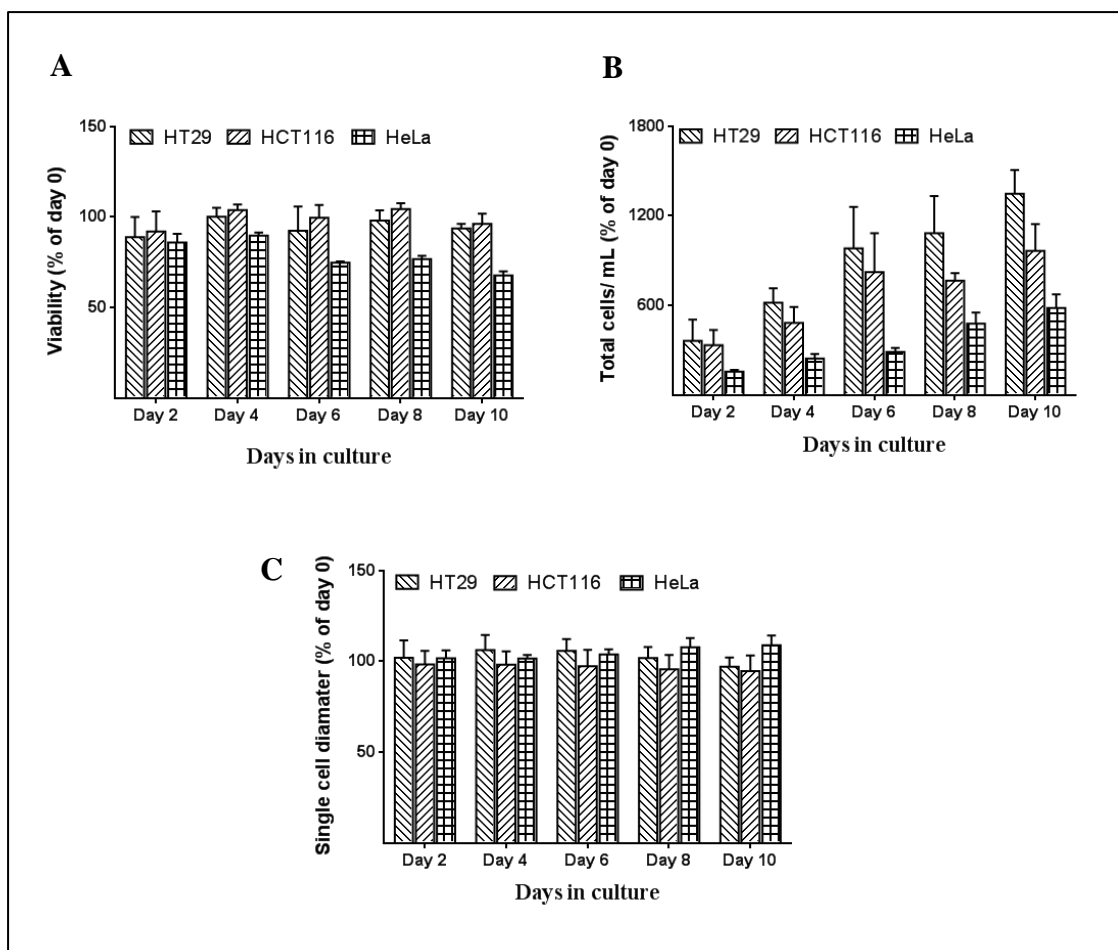


Figure 11: Changes in the (A) viability, (B) total cell number and (C) single-cell diameter in HCT116, HT29 and HeLa MCTS of size  $2.5 \times 10^4$  cell/mL with culture time. Data are the mean  $\pm$  SEM, n = 3.

### 3.3 Cell cycle changes in 3D cultures over time

To determine the cell cycle changes in 3D cultures, untreated MCTS of HCT116, HT29 and HeLa cells were collected every 3 days for 9 days and analyzed by flow cytometer.

Majority of cells in MCTS of HCT116 are in the  $G_0/G_1$  phase of the cell cycle. With increase in culture period, there is an increase in the accumulation of cells in this phase. On the other hand, there is a decrease in the number of cells in S and  $G_2/M$  phase with increase in MCTS size (Figure 12A).

Similarly to HCT116, we observed that a large percentage of cells in HT29 MCTS are in  $G_0/G_1$ . However, the number of cells in sub- $G_0$  (apoptotic cells) and  $G_0/G_1$  are very low on day 6 and 9, indicating that a significant number of cells undergo apoptosis on day 6 and 9 (Figure 12B). The numbers of cells in S phase and  $G_2/M$  phase decrease with increasing day of growth of MCTS.

Majority of cells in HeLa MCTS were in  $G_0/G_1$  phase only on day 0. The population of cells in sub- $G_0$  increases with increase in culture time. Interestingly, the most of cells from day 3 are located in apoptosis.

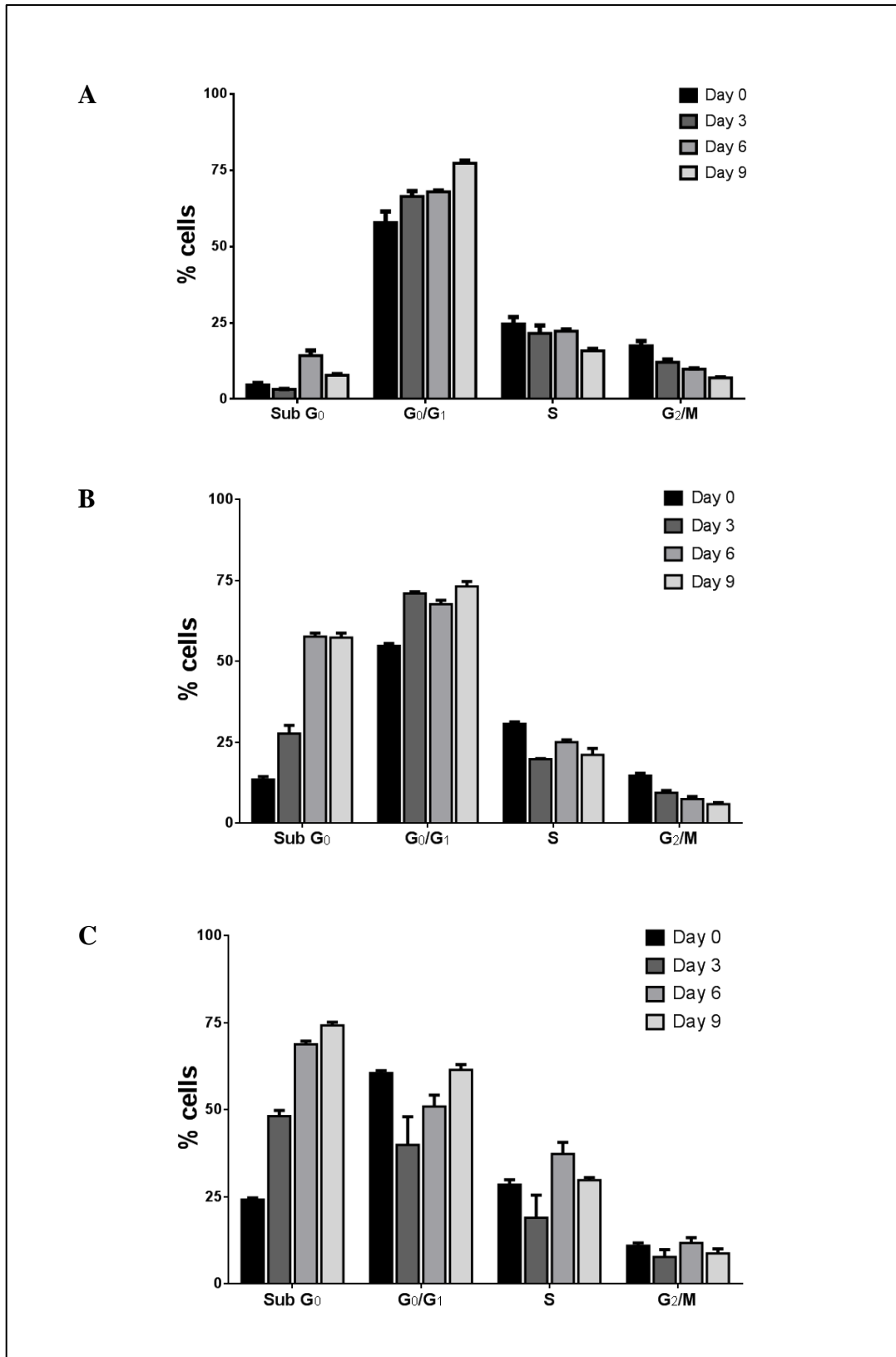


Figure 12: Bar graphs of changes in the cell cycle with growth of MCTS of (A) HCT116, (B) HT29 and (C) HeLa cells over 9 days in culture. Data are the mean  $\pm$  SEM,  $n = 3$ .

### 3.4 Changes in the expression of CAIX and HIF-1 $\alpha$ in 3D culture

To determine the growth-dependent change in the expression of CAIX and HIF-1 $\alpha$  over time, Western blotting was performed on protein lysates of HeLa, HCT116 and HT29 MCTS at Day 0, 3 and 6. CAIX and HIF-1 $\alpha$  are two intracellular proteins that regulate tumor pH and hypoxia, respectively. These proteins affect many cell signaling pathways and any change in their expression can potentially affect 3D culture response to anticancer drugs.

The expression of both proteins is low in HeLa MCTS culture during growth compared to colorectal cell lines. The level of CAIX decreases slightly on Day 3 in both colorectal cell lines, however, goes up to origin level on Day 6. The protein level of HIF-1 $\alpha$  decreases during growth of MCTS (Figure 13).

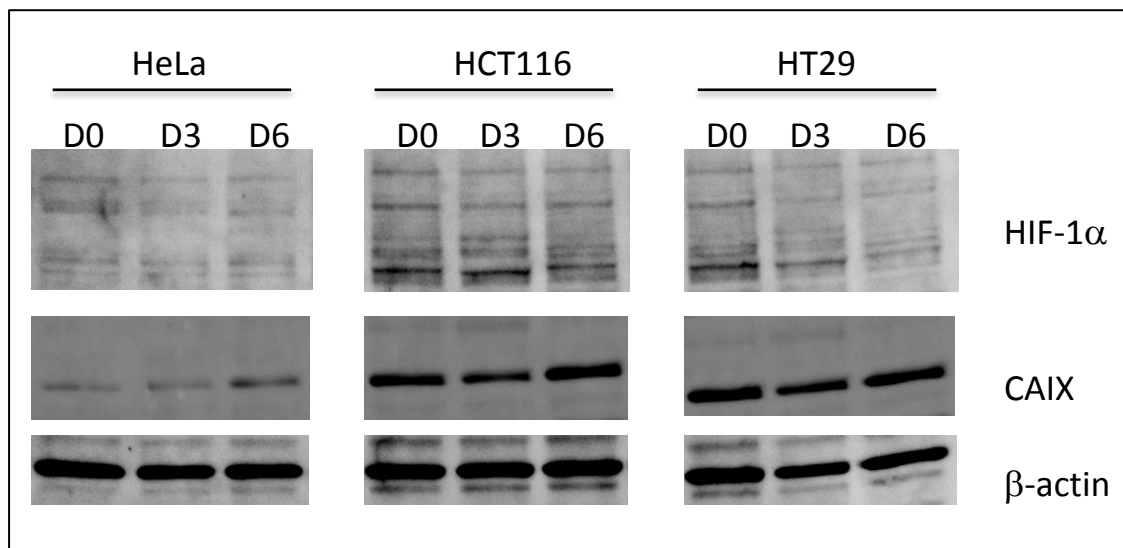


Figure 13: Representative Western blots of CAIX and HIF-1 $\alpha$  in MCTS of HeLa, HCT116 and HT29 cells. At least 30 MCTS per condition per cell line were collected on Day 0, 3 and 6, and lysed to perform WB. Multiple bands seen with HIF-1 $\alpha$  could possibly be due to its posttranslational modification.

### 3.5 Discussion

The results in general show that small-sized MCTS of each cell lines are grow better than large-sized spheroids. Furthermore, large-sized MCTS are not only incapable of continuous growth, but its growth even delay or completely stopped in a certain day of growth. From our data, we observed that MCTS with starting cell density of  $2.5 \times 10^4$  cells/mL are maintain a healthy condition and exponentially for 10 days without significant cell viability changes. The growth of bigger MCTS is significantly slow or stops completely after attaining a certain size. This applies to all cell lines.

This was confirmed by cell viability analysis experiments. These experiments show the highest increase of total cells and viable cells in size  $2.5 \times 10^4$ , while other sizes have lower increase, in the order of hundreds, in all cell lines. The viability decreases slightly from day 6 of growth, which may suggest the hypothesis from previous microscope experiment, that the MCTS after reaching a certain size slow down the growth of volume and/or completely stop growing.

Cell cycle analysis shows that with increase in MCTS volume, there is an increase in the number of cells in  $G_0/G_1$  phase (quiescent phase), and a simultaneous decrease in  $G_2/M$  cells (proliferating phase) in HCT116 cells. In HT29, the number of cells in  $G_0/G_1$  phase increases during the days of growth of MCTS, while decreases in  $G_2/M$  phase, as well as HCT116. However, a large number of cells in MCTS of HT29 are in apoptotic phase (sub- $G_0$ ) on day 6 and 9. These results may support the hypothesis that MCTS slow down the growth during the time of growth, because most of them are located in quiescent phase. On the other side, the data of HeLa cell line shows the increase of number of cells in apoptotic phase during the increase of time of growth, while the number of cells in other phases decreases during the time of growth.

The number of cells is similar in all cell lines in day 0. The number of cells in other days is variable in relation to cell line and phase of cell cycle. There is a difference between location in cell cycle in colorectal cancer cell lines and HeLa control cell line.

## 4. RESULT 2

We selected  $2.5 \times 10^4$  cell/mL and 6-day culture period as the appropriate MCTS growth condition for our system and tested a few standard anticancer agents on 3D cultures and compared the effects to 2D cultures. MTT cytotoxicity assay was performed only on 2D and 3D cultures of HCT116 cells. To determine the drug-induced changes on cell cycle, 2D and 3D cultures of both HCT116 and HT29 cells were analyzed by flow cytometer. Changes in the expression of apoptosis-related proteins in drug-treated 3D and 2D cultures were determined by Western blotting in HCT116 and HT29 cells. No drug treatment experiments were performed with 3D and 2D cultures of HeLa cells.

### 4.1 MTT Assay

HCT116 showed altered response to drugs in 2D and 3D cultures. Drugs such as, doxorubicin, gemcitabine, irinotecan and paclitaxel had higher  $IC_{50}$  values in 3D than 2D cultures (Figure 14). However, cisplatin, 5-fluorouracil, and vincristine were more effective in 3D and had lower  $IC_{50}$  values than 2D cultures (Figure 14). The  $IC_{50}$  of cisplatin, 5-fluorouracil and vincristine were  $1.57 \pm 0.38 \mu\text{g/mL}$ ,  $0.04 \pm 0.01 \mu\text{g/mL}$  and  $0.0028 \pm 0.0003 \mu\text{g/mL}$  in 3D cultures compared to  $0.05 \pm 0.01 \mu\text{g/mL}$ ,  $0.20 \pm 0.05 \mu\text{g/mL}$  and  $0.008 \pm 0.001 \mu\text{g/mL}$  in 2D cultures, respectively. All drugs resulted in 100% cell death in 2D; however, were unable to induce complete cell death in 3D cultures (Figure 14). Vincristine and paclitaxel, the two mitotic inhibitors, had minimal cell killing effects in 3D cultures, with nearly 50% surviving cells at a concentration as high as  $10 \mu\text{g/mL}$  (Figure 14 F, G). Interestingly, although vincristine had lower  $IC_{50}$  value in 3D cultures, it was unable to induce complete cell death in 3D compared to 2D cultures (Figure 14 G). The highest cytotoxic activity in 2D culture is seen with vincristine, paclitaxel and doxorubicin with  $IC_{50}$  values of  $0.008 \pm 0.001 \mu\text{g/mL}$ ,  $0.0032 \pm 0.0002 \mu\text{g/mL}$  and  $0.009 \pm 0.001 \mu\text{g/mL}$ , respectively. Although it appears that 2D and 3D cultures are sensitive to same drugs, it is important to note the difference between concentrations that had cytotoxicity effects. Paclitaxel acts at lower concentration in 2D cultures, while vincristine is effective in lower concentration in 3D cultures.



Similar results were obtained in 2D and 3D cultures of HT29 cells with these drugs. The experiments were performed by Mgr. Viswanath Das, Ph.D., and therefore the data are not shown in this thesis. The data from MTT assay on 2D and 3D cultures was presented at the X. Diagnostic, Predictive and Experimental Oncology Days conference in Olomouc, Czech Republic in Dec 2014 (Appendix III).

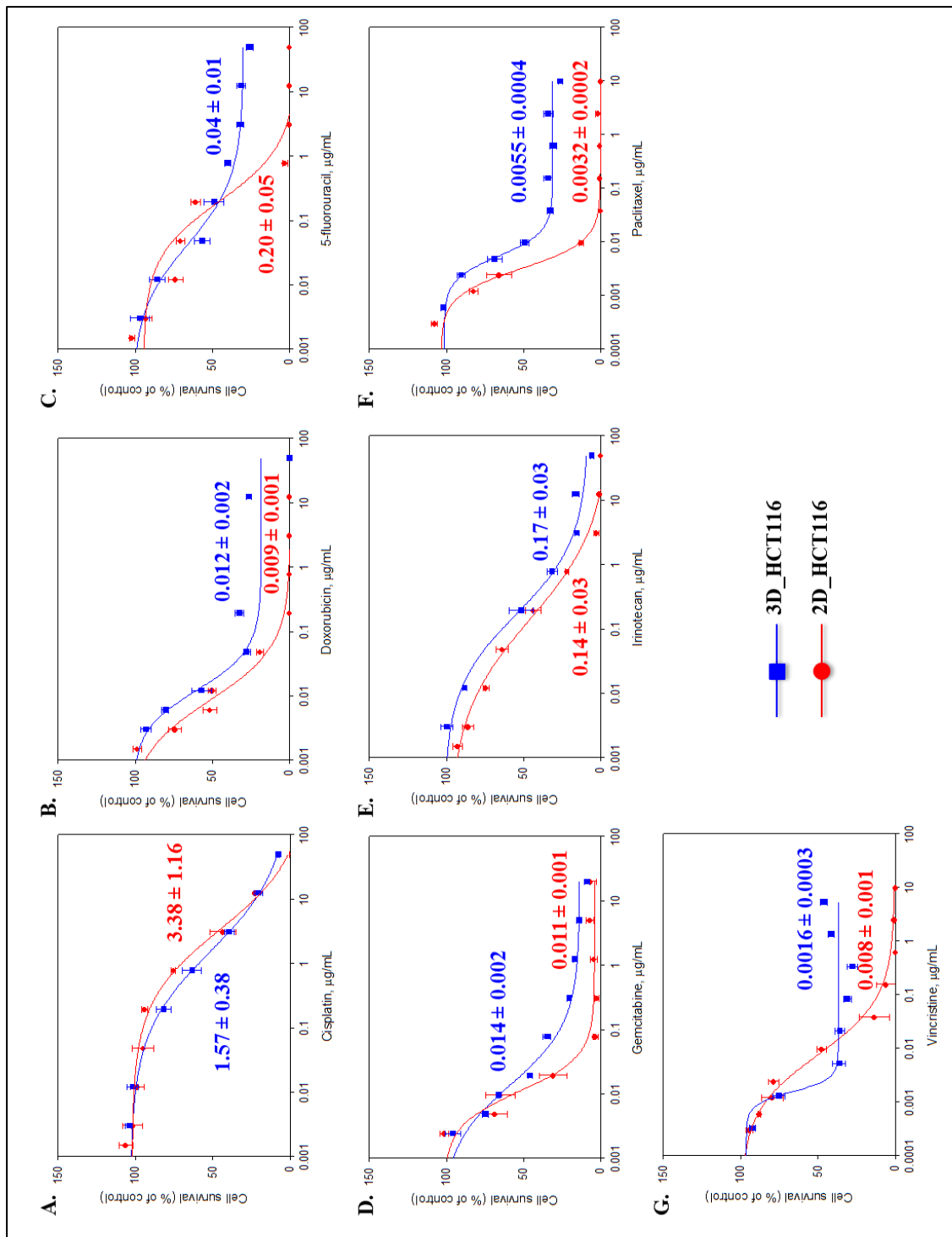


Figure 14: Dose-response curves of anticancer drugs in 2D (red lines) and 3D (blue lines) cultures of HCT116 cells. The IC<sub>50</sub> ± SD of each drug in µg/mL are shown next to their respective curves.

## 4.2 Cell cycle changes in 2D and 3D culture using treatment

Vincristine and paclitaxel resulted in an increased G<sub>2</sub>/M block in 2D cultures compared to controls, but did not induce much change in 3D cultures compared to 2D. A similar increase in G<sub>2</sub>/M block is also seen in 2D cultures with doxorubicin, gemcitabine, and irinotecan in both the cell types. Interestingly, irinotecan and cisplatin caused an increased accumulation of cells in the S phase in 2D compared to 3D cultures of both the cell lines. Additionally, compared to untreated 3D HCT116 and HT29 cultures, treatment with all drugs resulted in an increase in the percent of cells in G<sub>0</sub>/G<sub>1</sub>. This effect is, however, not seen in 2D cultures of the same cell types. There appears no effect of drugs on cells in G<sub>0</sub>/G<sub>1</sub> phase in 3D cultures. Treatment of 3D cultures also resulted in an increase in sub-G<sub>0</sub> apoptotic cells compared to 3D controls. This effect is not observed in the 2D cultures, and the fraction of cells in sub-G<sub>0</sub> apoptotic phase in 2D cultures following treatment showed no change compared to untreated 2D samples (Figure 15, 16).

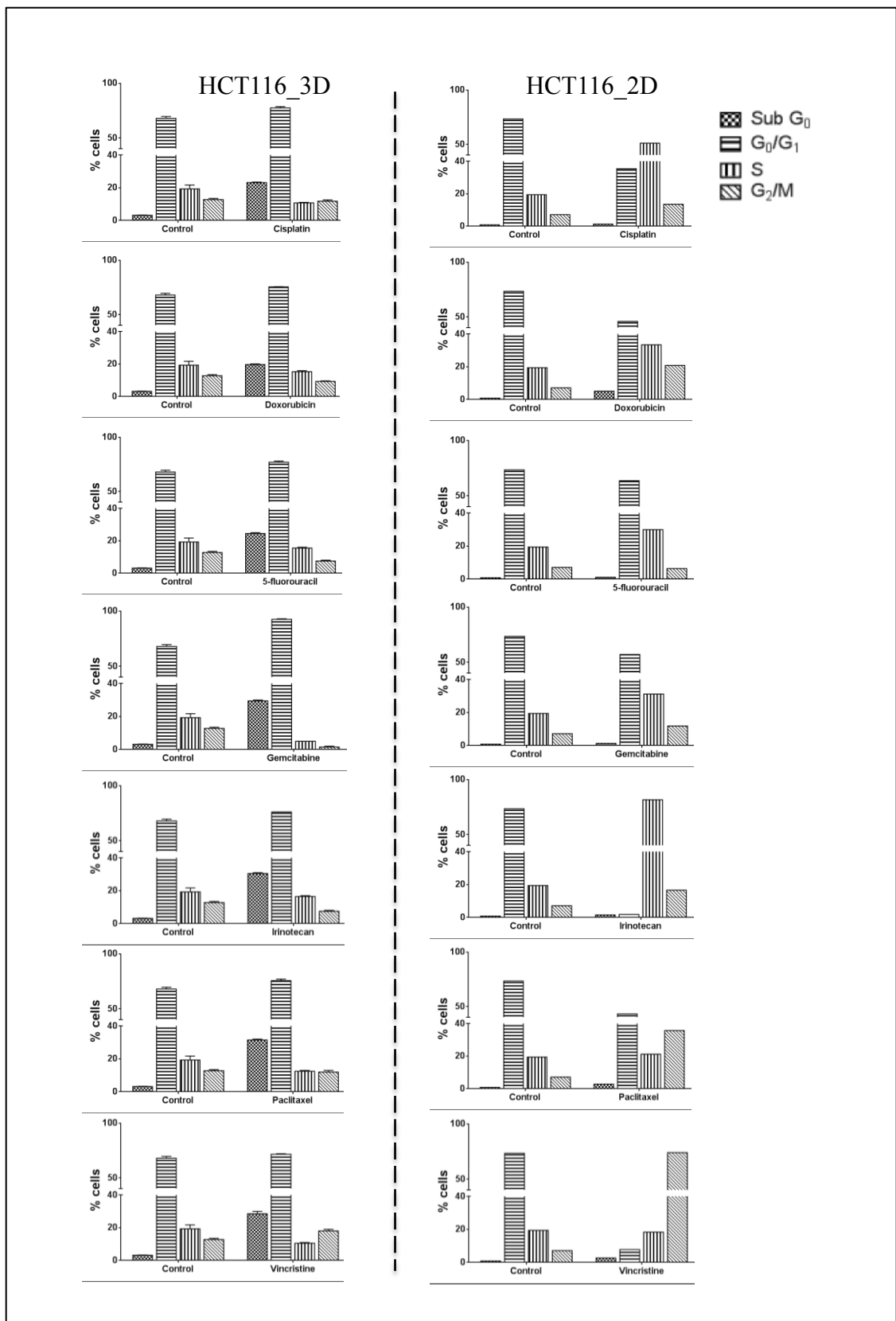


Figure 15: Effect of cytotoxic drugs on the cell cycle of HCT116 cells cultured in 3D and 2D determined by flow cytometry. Data are shown as mean  $\pm$  SEM, n = 2.

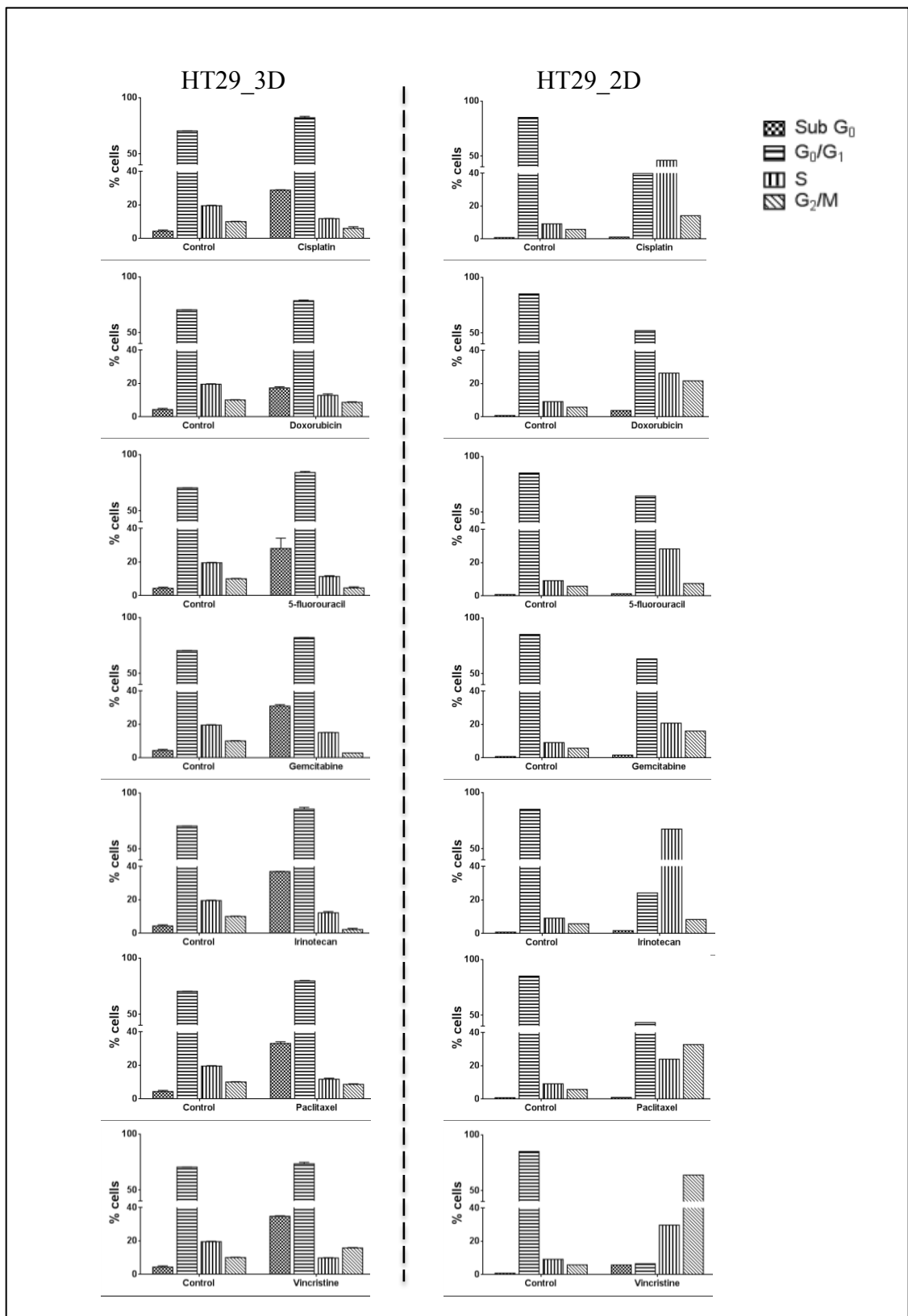


Figure 16: Cytotoxic effect of selected drugs on the cell cycle of 3D and 2D cultures HT29 cells line using flow cytometry. Data are shown as mean  $\pm$  SEM,  $n = 2$ .

### **4.3 Changes in the expression of N-myc, caspase 8 and CAIX in 2D and 3D cultures**

To further study the effect of anticancer cancer drugs on 2D and 3D cultures of HCT116 and HT29 cells, we performed Western blot on drug-treated sample and stained for N-myc and caspase 8. We also stained for CAIX to see if there are any drug-induced changes in its expression. There was no change in the expression levels of proto-oncogene protein N-myc following drug treatment between 2D and 3D cultures. However, low expression of pro-apoptotic protein Caspase 8 is seen in 3D cultures of both the cell lines following drug treatment. Caspase 8 is a marker of apoptosis. Its expression in 3D cultures presumably confirms the our cell cycle results in 3D where we observed an increased apoptosis following drug treatment compared to 2D cultures. CAIX expression is low in the 2D samples treated with cisplatin, doxorubicin and 5-fluorouracil than gemcitabine and irinotecan in HCT116. Treatment with paclitaxel resulted in low CAIX levels in 3D cultures of HCT116 and HT29 cells (Figure 17).

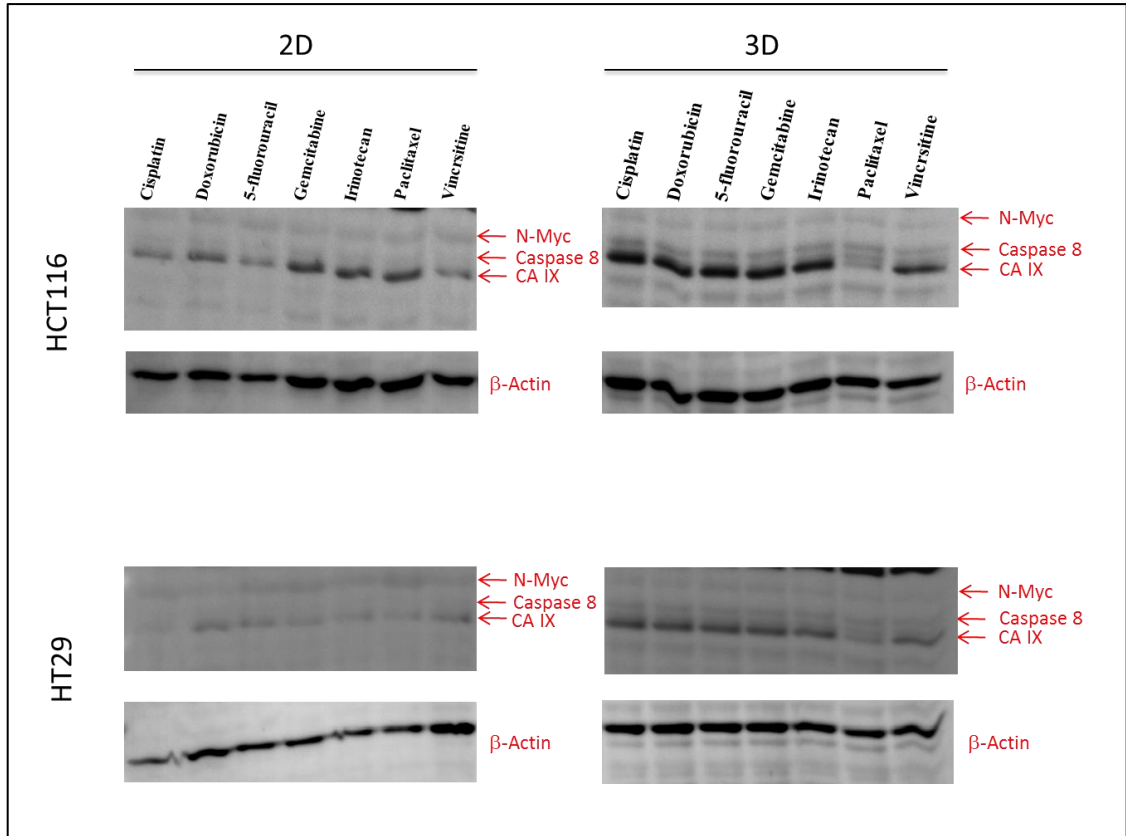


Figure 17: The expression of selected proteins in 2D and 3D culture in HCT116 and HT29 cell line.

#### 4.4 Discussion

We have shown that drugs resulted in 100% cell death in 2D cultures, fail to do so in 3D cultures of HCT116 cells. It is interesting to note that cisplatin, 5-fluorouracil and vincristine were more effective in 3D cultures, and had lower IC<sub>50</sub> values compared to 2D. On the other hand, 3D cultures were highly resistant to doxorubicin, gemcitabine, irinotecan and paclitaxel with high IC<sub>50</sub> values. The highest cytotoxic effect in 2D culture was observed in vincristine, paclitaxel and doxorubicin treated cells. Although it seems that both cultures are sensitive to same drugs, it is necessary to see the difference between concentrations at which cytotoxicity is observed. These differences in 2D and MCTS cultures to drug response can result from many reasons. Cell signaling pathways differ between 2D and 3D cultures of cells (Fatima et al., 2008), and alter response of cells to anticancer drugs in 2D and 3D microenvironment.

Mitotic drugs, such as vincristine and paclitaxel resulted in high G<sub>2</sub>/M block in 2D culture compared to 3D, possibly due the presence of high non-mitotic cells in 3D cultures. Cisplatin and irinotecan effects are primarily seen in S phase in 2D culture compared to MCTS. These two drugs are inhibitors of DNA replication. Irinotecan is topoisomerase inhibitor and works in the S phase of dividing cells in 2D culture, while cisplatin is an alkylating agent, which is cell cycle independent. All drugs affect the cells in G<sub>0</sub>/G<sub>1</sub> phase in 3D culture compared to control. Moreover, all these drugs increase the apoptosis in 3D culture.

Due to time constrains, Western blot experiments to study the effect of drugs on the expression of N-myc, caspase 8 and CAIX could not be repeated more than once, and therefore, it would be inappropriate to make premature conclusions. However, it is possible to see that lower expression of caspase 8 in 2D than in 3D cultures following drug treatment. This can potentially confirm that higher apoptosis in 3D from previous experiment, because caspase 8 is pro-apoptotic protein.



## 5. CONCLUSION

The aims of this thesis were to determine the suitable conditions for culturing of HCT116 and HT29 cells in 3D as MCTS for use in high throughput screening of anticancer drugs in our laboratory. Our results show that MCTS formed with low cell number ( $2.5 \times 10^4$  cells/mL) grow and maintain a healthy condition up to 10 days in culture. There are no major changes in these MCTS that can affect cell response to drugs due to the presence of unhealthy cells. The MCTS formed in bigger sizes are unable to grow continuously, and reach a plateau within a few days that can affect cell response to drugs.

The second aim of the thesis was to study the effect of a few selected anticancer drugs on MCTS cultured under the selected growth conditions from Aim 1, and compare the effects to 2D cultures. This experiment was performed by MTT test on MCTS and 2D culture. Subsequently, the cell cycle analysis of treated MCTS and 2D culture was completed and, finally, the level of expression of selected apoptotic and hypoxia-associated proteins after treatment was determined. It was confirmed that some drugs are cytotoxic in 2D culture and some in 3D cultures. It may be due to altered cell cycle between 2D and 3d cultures, and/or changes in the level of hypoxia and acidity in 3D cultures. Due to time constrains, a few experiments were performed only once. One of the important tasks in the future would be repeat the experiments to increase the n value to confirm the preliminary findings of this thesis. Additionally studies are also required to characterize the drug-induced changes in 3D cultures.

## REFERENCES

- ANDRÉ, T., BONI, C., MOUNEDJI-BOUDIAF, L., NAVARRO, M., TABERNERO, J., HICKISH, T., TOPHAM, C., ZANINELLI, M., CLINGAN, P., BRIDGEWATER, J., TABAH-FISCH, I., de GRAMONT, A.: Oxaliplatin, Fluorouracil, and Leucovorin as Adjuvant Treatment for Colon Cancer. *New England Journal of Medicine*. 2004, 350: 2343-2351.
- AOUDJIT, F. and VUORI, K.: Integrin Signaling in Cancer Cell Survival and Chemoresistance. *Chemotherapy Research and Practice*. 2012, 2012: 1-16.
- ARNOLD, C. N., GOEL, A., BLUM, H. E., BOLANT, C. R.: Molecular Pathogenesis of Colorectal Cancer: Implications for Molecular Diagnosis. *Cancer*. 2005, 104: 2035-2047.
- BAKER, B. M., CHEN, C. S., GILLETTE, B. M., PARSA, H., SIA, S. K.: Deconstructing the third dimension - how 3D culture microenvironments alter cellular cues. *Journal of Cell Science*. 2012, 125: 53-79.
- BRESLIN, S. and O'DRISCOLL, L.: Three-dimensional cell culture: the missing link in drug discovery. *Drug Discovery Today*. 2013, 18: 240-249.
- COWAN, D. S. M. and TANNOCK, I. F.: Factors that influence the penetration of methotrexate through solid tissue. *International Journal of Cancer*. 2001, 91: 120-125.
- DAS, V., ŠTĚPÁNKOVÁ, J., HAJDÚCH, M., MILLER, J. H.: Role of tumor hypoxia in acquisition of resistance to microtubule-stabilizing drugs. *Biochimica et Biophysica Acta (BBA) - Reviews on Cancer*. 2015, 1855: 172-182.
- DELCO, F. and SONNENBERG, A.: Limitations of the faecal occult blood test in screening for colorectal cancer. *Italian Journal of Gastroenterology and Hepatology*. 1999, 31.
- DIETVORST, M. H. P. and ESKENS, F. A. L. M.: Current and Novel Treatment Options for Metastatic Colorectal Cancer: Emphasis on Aflibercept. *Biologics in Therapy*. 2013, 3: 25-33.

DONG, X. and MUMPER, R. J.: Nanomedicinal strategies to treat multidrug-resistant tumors: current progress. *Nanomedicine*. 2010, 5: 71-87.

FATIMA, N., YI, M., AJAZ, S., STEPHENS, R. M., STAUFFER, S., GREENWALD, P., MUNROE, D. J., ALI, I. U.: Altered Gene Expression Profiles Define Pathways in Colorectal Cancer Cell Lines Affected by Celecoxib. *Cancer Epidemiology, Biomarkers and Prevention*. 2008, 17: 3051-3061.

FRIEDRICH, J., EDER, W., CASTANEDA, J., DOSS, M., HUBER, E., EBNER, R., KUNZ-SCHUGHART, L. A.: A Reliable Tool to Determine Cell Viability in Complex 3-D Culture: The Acid Phosphatase Assay. *Journal of Biomolecular Screening*. 2007, 12: 925-937.

GERWECK, L. E.: Tumor pH controls the in vivo efficacy of weak acid and base chemotherapeutics. *Molecular Cancer Therapeutics*. 2006, 5: 1275-1279.

GILLET, J.P. and GOTTESMAN, M. M.: Mechanisms of multidrug resistance in cancer. *Methods in Molecular Biology*. 2010, 596: 47-76.

GOLDBERG, R. M., SARGENT, D. J., MORTON, R. F., FUCHS, C. S., RAMANATHAN, R. K., WILLIAMSON, S. K., FINDLAY, B. P., PITOT, H. C., ALBERTS, S. R.: A Randomized Controlled Trial of Fluorouracil Plus Leucovorin, Irinotecan, and Oxaliplatin Combinations in Patients With Previously Untreated Metastatic Colorectal Cancer. *Journal of Clinical Oncology*. 2004, 22: 23-30.

GRIMM, M., CETINDIS, M., LEHMANN, M., BIEGNER, T., MUNZ, A., TERIETE, P., KRAUT, W., REINERT, S.: Association of cancer metabolism-related proteins with oral carcinogenesis – indications for chemoprevention and metabolic sensitizing of oral squamous cell carcinoma?. *Journal of Translational Medicine*. 2014, 12: 1-21.

HAGGAR, F., BOUSHEY, R., LEMMENS, V. E. P. P., COEBERGH, J.-W. W.: Colorectal Cancer Epidemiology: Incidence, Mortality, Survival, and Risk Factors. *Clinics in Colon and Rectal Surgery*. 2009, 22: 1-17.

HICKMAN, J. A., GRAESER, R., de HOOGT, R., VIDIC, S., BRITO, C., GUTEKUNST, M., van der KUIP, H.: Three-dimensional models of cancer for

pharmacology and cancer cell biology: Capturing tumor complexity in vitro/ex vivo. *Biotechnology Journal*. 2014, 9: 1115-1128.

HIRSCH, B. R. and ZAFAR, S. Y.: Capecitabine in the management of colorectal cancer. *Cancer Management and Research*. 2011, 3: 79-89.

HIRSCHHAEUSER, F., MENNE, H., DITTFELD, C., WEST, J., MUELLER-KLIESER, W., KUNZ-SCHUGHART L. A.: Multicellular tumor spheroids: An underestimated tool is catching up again. *Journal of Biotechnology*. 2010, 148: 3-15.

HORWITZ, S.B.: Taxol (paclitaxel): mechanisms of action. *Annals of Oncology*. 1994, 5: 3-6.

JABLONSKÁ M. et kol.: Kolorektální karcinom - časná diagnóza a prevence. First edition. *GRADA Publishing, spol. s r. o.*, 2000. ISBN 80-7169-777-X.

JEMAL, A., BRAY, F., CENTER, M. M., FERLAY, J., WARD, E., FORMAN, D.: Global cancer statistics. *CA: A Cancer Journal for Clinicians*. 2011, 61: 69-90.

LABIANCA, R., NORDLINGER, B., BERETTA, G. D., BROUQUET, A., CERVANTES, A., and On behalf of the ESMO Guidelines Working GROUP.: Primary colon cancer: ESMO Clinical Practice Guidelines for diagnosis, adjuvant treatment and follow-up. *Annals of Oncology*. 2010, 21: 70-77.

LAURENT, J., FRONGIA, C., CAZALES, M., MONDESERT, O., DUCOMMUN, B., LOBJOIS, V.: Multicellular tumor spheroid models to explore cell cycle checkpoints in 3D. *BMC Cancer*. 2013, 13.

LOBRY, C., OH, P., AIFANTIS, I.: Oncogenic and tumor suppressor functions of Notch in cancer: it's NOTCH what you think. *The Journal of Experimental Medicine*. 2011, 208: 1931-1935.

LORENZO, C., FRONGIA, C., JORAND, R., FEHRENBACH, J., WEISS, P., MAANDHUI, A., GAY, G., DUCOMMUN, B., LOBJOIS, V., PAMPALONI, F., RICHA, R., ANSARI, N., STELZER, E. H. K.: Live cell division dynamics monitoring in 3D large spheroid tumor models using light sheet microscopy. *Cell Division*. 2011, 6: 43-57.

- LOWENFELS, A.B.: Fecal occult blood testing as a screening procedure for colorectal cancer. *Annals of Oncology*. 2002, 13: 40-43.
- LU, H.-P. and CHAO, C. C. K.: Cancer Cells Acquire Resistance to Anticancer Drugs: An Update. *Biomedical Journal*. 2012, 35: 464-472.
- LUCA, A. C., MERSCH, S., DEENEN, R., SCHMIDT, S., MESSNER, I., SCHÄFER, K.-L., BALDUS, S. E., HUCKENBECK, W., PIEKORZ, R. P., KNOEFEL, W. T., KRIEG, A., STOECKLEIN, N. H.: Impact of the 3D Microenvironment on Phenotype, Gene Expression, and EGFR Inhibition of Colorectal Cancer Cell Lines. *PLoS ONE*. 2013, 8.
- MARKOWITZ, S. D. and BERTAGNOLLI, M. M.: Molecular Basis of Colorectal Cancer. *New England Journal of Medicine*. 2009, 361: 2449-2460.
- MOHAMMADGHOLI, A., RABBANI-CHADEGANI, A., FALLAH, S.: Mechanism of the Interaction of Plant Alkaloid Vincristine with DNA and Chromatin: Spectroscopic Study. *DNA and Cell Biology*. 2013, 32: 228-235.
- NELSON, H., PETRELLI, N., CARLIN, A., COUTURE, J., FLESHMAN, J., GUILLEM, J., MIEDEMA, B., OTA, D., SARGENT, D.: Guidelines 2000 for Colon and Rectal Cancer Surgery. *Journal of the National Cancer Institute*. 2001, 93: 583-596.
- O'CONNELL, J. B., MAGGARD, M. A., KO, C. Y.: Colon Cancer Survival Rates With the New American Joint Committee on Cancer Sixth Edition Staging. *Journal of the National Cancer Institute*. 2004, 96: 1420-1425.
- PLUNKETT, W., HUANG, P., GANDHI, V.: Preclinical characteristics of gemcitabine: Relevance for Clinical Studies. *Anti-Cancer Drugs*. 1995, 6: 11-19.
- SAUER, R., BECKER, H., HOHENBERGER, W., RÖDEL, C., WITTEKIND, C., FIETKAU, R., MARTUS, P., TSCHMELITSCH, J., HAGER, E., HESS, C. F., KARSTENS, J. H., LIERSCH, T., SCHMIDBERGER, H., RAAB, R.: Preoperative versus Postoperative Chemoradiotherapy for Rectal Cancer. *New England Journal of Medicine*. 2004, 351: 1731-1740.

SCHMIEDER, R., HOFFMANN, J., BECKER, M., BHARGAVA, A., MÜLLER, T., KAHMANN, N., ELLINGHAUS, P., ADAMS, R., ROSENTHAL, A., THIERAUCH, K.-H., SCHOLZ, A., WILHELM, S. M., ZOPF, D.: Regorafenib (BAY 73-4506): Antitumor and antimetastatic activities in preclinical models of colorectal cancer. *International Journal of Cancer*. 2014, 135: 1487-1496.

SHI, S., YAO, W., XU, J., LONG, J., LIU C., YU, X.: Combinational therapy: New hope for pancreatic cancer? *Cancer Letters*. 2012, 317: 127-135.

SIDDIK, Z. H.: Cisplatin: mode of cytotoxic action and molecular basis of resistance. *Oncogene*. 2003, 22: 137-173.

STRAUSSMAN, R., MORIKAWA, T., SHEE, K., BARZILY-ROKNI, M., RONG QIAN, Z., DU, J., DAVIS, A., MONGARE, M. M., GOULD, J., FREDERICK, D. T., COOPER, Z. A., CHAPMAN, P. B., SOLIT, D. B., RIBAS, A., LO, R. S., FLAHERTY, K. T., OGINO, S., WARGO, J. A., GOLUB, T. R.: Tumour micro-environment elicits innate resistance to RAF inhibitors through HGF secretion. *Nature*. 2012, 487: 500-504.

TANNOCK, I. F., LEE, C. M., TUNGALL, J. K., COWAN, D. S. M., EGORIN, M. J.: Limited Penetration of Anticancer Drugs through Tumor Tissue: A Potential Cause of Resistance of Solid Tumors to Chemotherapy. *Clinical Cancer Research*. 2002, 8: 878-884.

THORN, C. F., OSHIRO, C., MARSH, S., HERNANDEZ-BOUSSARD, T., MCLEOD, H., KLEIN, T. E., ALTMAN, R. B.: Doxorubicin pathways: pharmacodynamics and adverse effects. *Pharmacogenetics and Genomics*. 2011, 21: 440-446.

TRÉDAN, O., GALMARINI, C. M., PATEL, K., TANNOCK, I. F.: Drug Resistance and the Solid Tumor Microenvironment. *Journal of the National Cancer Institute*. 2007, 99: 1441-1454.

TSANG, A. H.-F., CHENG, K. H., WONG, A. S.-P., NG, S. S.-M., MA, B. B.-Y., CHAN, C. M.-P., TSUI, N. B.-Y., WING-CHICHAN, L., YUNG, B. Y.-M., WONG,

S.-C. C.: Current and future molecular diagnostics in colorectal cancer and colorectal adenoma. *World Journal of Gastroenterology*. 2014, 20: 3847-3857.

VINOGRADOV, S. and WEI, X.: Cancer stem cells and drug resistance: the potential of nanomedicine. *Nanomedicine*. 2012, 7: 597-615.

WENZEL C., RIEFKE, B., GRÜNDEMANN, S., KREBS, A., CHRISTIAN, F., PRINZ, S., OSTERLAND, M., GOLFIER, S., RÄSE, S., ANSARI, N., ESNER, M., BICKLE, M., PAMPALONI, F., MATTHEYER, C., STELZER, E. H., PARCZYK, K., PRECHTL, S., STEIGEMANN, P.: 3D high-content screening for the identification of compounds that target cells in dormant tumor spheroid regions. *Experimental Cell Research*. 2014, 323: 131-143.

XU, Y. and VILLALONA-CALERO, M. A.: Irinotecan: mechanisms of tumor resistance and novel strategies for modulating its activity. *Annals of Oncology*. 2002, 13: 1841-1851.

YOKOMIZO, H., YOSHIMATSU, K., OTANI, T., OSAWA, G., NAKAYAMA, M., MATSUMOTO, A., YANO, Y., OKAYAMA, S., NARITIKA, Y.: Practical use of Capecitabine plus Oxaliplatin (CAPEOX) with Bevacizumab for Patients with Metastatic Colorectal Cancer that cannot Expect Conversion Therapy. *Hepato-Gastroenterology*. 2013, vol. 60.

ZOUHAIRI, M. E., CHARABATY, A., PISHVAIAN, M. J.: Molecularly Targeted Therapy for Metastatic Colon Cancer: Proven Treatments and Promising New Agents. *Gastrointestinal Cancer Research*. 2011, 4: 15-21.

## APPENDIX I

### STOCKS:

**PBS:** 137 mM NaCl, 1.6 mM KCl, 10 mM Na<sub>2</sub>HPO<sub>4</sub>\*12H<sub>2</sub>O, 1.8 mM KH<sub>2</sub>PO<sub>4</sub> (pH=7.4)

**PBST:** PBS + 0.1% Tween 20

**Lysis buffer:** 20 mM Tris-HCl (pH=8), 137 mM NaCl, 10% glycerol, 1% Nonidet P40 (Cat. # 74385, Sigma), 2 mM EDTA, protease (1 tablet/mL; Cat. # 04693116001, Hoffmann-La Roche AG, Basel, Switzerland) and phosphatase inhibitors (1 tablet/mL, Cat. # 04906837001, Hoffmann-La Roche AG)

**5× SDS loading buffer:** 250 mM Tris-HCl (pH=6.8), 10% SDS, 30% glycerol, 0.5 M DTT (Cat. # D0632, Sigma-Aldrich), 0.02% Bromophenol Blue, 10% Mercaptoethanol (Cat. # M6250, Sigma-Aldrich)

**Blocking solution:** 5 g BSA (Cat. # A2153, Sigma-Aldrich) in 100 mL PBST

**MTT stock:** 5 mg MTT (Cat. # M2128, Sigma-Aldrich) in 1 mL sterile PBS and filtered. Stored at -20°C.

**Citrate buffer:** 5.68 g sodium citrate tribasic monohydrate (Cat. # C8532, Sigma-Aldrich) in 500 mL deionized water

**Propidium iodide:** 2 mg propidium iodide (Cat. # 81845, Sigma- Aldrich), 4 mL 2% Triton X-100 (Cat. # T8787, Sigma-Aldrich), 36 mL deionized water.

**10% Resolving gel:** 1.5 M Tris (pH=8.8), 10% SDS, 30% Acrylamide/Bis-acrylamide (Cat. # A2792, Sigma-Aldrich), 10% APS and TEMED in H<sub>2</sub>O

**4% Stacking gel:** 0.5 M Tris (pH=6.8), 10% SDS, 30% Acrylamide/Bis-acrylamide, 10% APS and TEMED in H<sub>2</sub>O

### **Agarose coating of plates**

1. Dissolve 0.75 g of low-melting agarose (Cat. # A9414, Sigma-Aldrich) in McCoy's or DMEM medium without supplement.



2. Heat to dissolve agarose and autoclave to sterilize.
3. Allow agarose solution to cool to 50-60°C, and then filter using a Nalgene™ Rapid-Flow™ Sterile Disposable Filter (pore size 0.45 µm; Cat. # 124-0045, Thermo Fisher Scientific, MA, USA).

Using a Multidrop™ Combi Reagent Dispenser add 50 µL/well to a 96-well plate, and 10-15µL/well to a 384-well plate.

## **EQUIPMENT:**

<b>Name</b>	<b>Company, Country</b>
<b>Axio Observer.D1 with AxioCamera MRC5</b>	Carl Zeiss, Germany
<b>BD FACSCalibur Cell Analyzer</b>	BD Biosciences, USA
<b>Centrifuge 5810R</b>	Eppendorf, Germany
<b>ChemiDoc MP analyzer</b>	BioRad, Austria
<b>EnSpire Multimode Plate Reader</b>	PerkinElmer Inc., USA
<b>EnVision Multimode Plate Reader</b>	PerkinElmer Inc., USA
<b>Hettich Rotina 420 R Centrifuge</b>	Hettich Zentrifugen, Germany
<b>Minicentrifuge</b>	National Labnet Co., USA
<b>Electrophoresis and Blotting Vertical Apparatus</b>	BioRad, Austria
<b>MSC-Advantage Biological Safety Cabinet (flow-box)</b>	Thermo Scientific, USA
<b>Olympus IX51 Microscope</b>	Olympus, Japan
<b>SteriStore Rotary Incubator</b>	HighRes Biosolution, USA
<b>ViCell XR Cell Viability Analyzer</b>	Beckman Coulter Inc., USA

## **CHEMICALS:**

<b>Chemical</b>	<b>Company</b>	<b>Catalog #</b>
<b>Accutase® solution</b>	Sigma-Aldrich	A6964
<b>Acrylamide/Bis-acrylamide</b>	Sigma-Aldrich	A2792
<b>Agarose, low melting</b>	Sigma-Aldrich	A9414
<b>Bovine serum albumin</b>	Sigma-Aldrich	A2153
<b>β-Mercaptoethanol</b>	Sigma-Aldrich	M6250
<b>Dithiothreitol (DTT)</b>	Sigma-Aldrich	D0632
<b>Nonidet P40</b>	Sigma-Aldrich	74385
<b>Propidium Iodide</b>	Sigma-Aldrich	81845
<b>Phosphatase Inhibitor Cocktail Tablets</b>	Roche	04906837001
<b>Protease Inhibitor Cocktail Tablets</b>	Roche	04693116001
<b>Thiazolyl Blue Tetrazolium Bromide (MTT)</b>	Sigma-Aldrich	M2128
<b>Tryple</b>	Life Technologies	12563-029

## **APPENDIX II**

### **ANTICANCER AGENTS:**

#### **Cisplatin**

Cytotoxic effect of cisplatin is based on interactions with DNA. Cisplatin binds to the DNA to form intrastrand crosslink DNA adducts, which activate several signaling pathways, including ATR (ataxia telangiectasia and Rad3-related protein), p53, p73 and MAPK. It leads to activation of apoptosis (Siddik, 2003).

#### **Doxorubicin**

Doxorubicin is antitumor antibiotic extracted from *Streptomyces peucetius var. caesius*. It works via two major mechanisms of action: intercalation into DNA and generation of free radicals. Intercalation into DNA causes DNA breaks and interferes to DNA synthesis. Interaction between DNA and doxorubicin may cause also poisoning of topoisomerase II. Generation of free radicals leads to cell membrane damage (Thorn et al., 2011).

#### **Fluorouracil**

Fluorouracil is an analog of pyrimidine base thymine of nucleic acids, where the methyl group of 5' carbon is replaced by fluor. This antimetabolite slows down DNA synthesis by inhibiting the thymidilate synthase that normally converts deoxyuridine monophosphate to deoxythymidine monophosphate, resulting in cell death (Jablonská et al., 2000).

#### **Gemcitabine**

This analog of deoxycytidine is antimetabolite, which have to be phosphorylated by deoxycytidine kinase to an active form: gemcitabine diphosphate and gemcitabine triphosphate. These active forms are able to be transported into the cell, where are incorporated into elongating DNA strand instead of deoxycytosintriphosphate (dCTP). It leads to arrest of DNA synthesis and mask of termination end with active form of gemcitabine, which do not allow the DNA repair (Plunkett et al., 1995).

**Irinotecan**

Irinotecan is camptothecin analog, derived from the tree *Camptotheca acuminata*. It inhibits topoisomerase I that controls the structure of DNA by relaxing the supercoiled DNA. Inhibition of topoisomerase I leads to DNA breaks, and eventually cell death (Xu & Villalona-Calero, 2002).

**Paclitaxel**

Paclitaxel is antitumor drug with specific binding site on the microtubule polymer and enhances the polymerization of tubulin to stable microtubules. It stabilizes them against depolymerization by cold and calcium. It culminates in stopping the cell cycle in G2/M and these cells are unable to form a normal mitotic apparatus (Horwitz, 1994).

**Vincristine**

Vincristine is antimicrotubule agent extracted from plants. The vinca alkaloids are isolated from *Catharanthus roseus*. That drug is cell-cycle specific. It means that affects cells only when they are dividing. Vincristine inhibits the microtubules necessary for dividing, which results in cell death (Mohammadgholi et al., 2013).

## APPENDIX III


XXI


Diagnostic,  
Predictive and  
Experimental  
ONCOLOGY  
Days

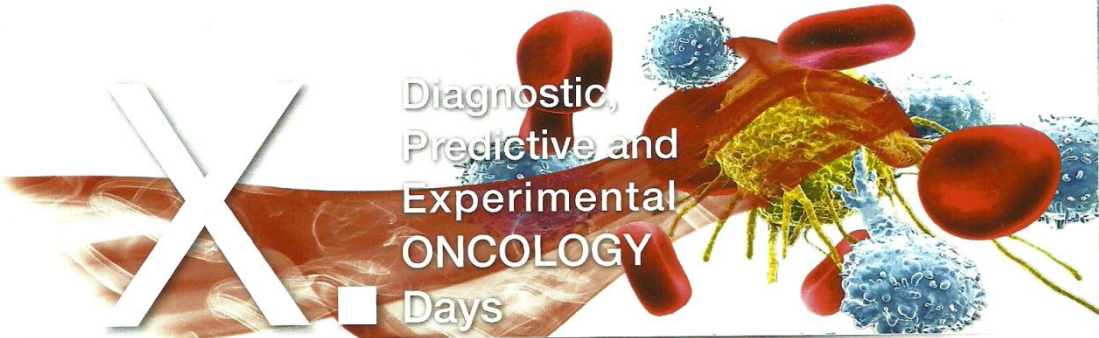
ABSTRACT BOOK

December 02 - 03, 2014  
hotel NH Collection Olomouc Congress  
Legionarska 21, 779 00 Olomouc,  
Czech Republic

[www.imtm.cz](http://www.imtm.cz)

 INSTITUTE OF MOLECULAR AND  
TRANSLATIONAL MEDICINE

 **MedChemBio**  
Cluster of Medical Chemistry and Chemical Biology



Diagnostic,  
Predictive and  
Experimental  
**ONCOLOGY**  
Days

**Pořadatel**

Ústav molekulární a translační medicíny LF UP a FN Olomouc  
Ústav klinické a molekulární patologie LF UP a FN Olomouc  
MedChemBio - zájmové sdružení právnických osob

**Odborná garance**

Sekce diagnostické a prediktivní onkologie České onkologické společnosti ČLS JEP  
Komplexní onkologické centrum Olomouc

**Prezident akce**

doc.MUDr. Marián Hajdúch, Ph.D.

**Organizační výbor**

doc. Mgr. Jiří Drábek, Ph.D., RNDr. Radek Trojanec Ph.D., MUDr. Kateřina Bouchalová, Ph.D.,  
MUDr. Petr Džubák, Ph.D., MUDr. Josef Srovnal, Ph.D., doc. RNDr. Ondřej Slabý, Ph.D.,  
doc. MUDr. Marek Svoboda, Ph.D.

**Organizátor**

Ústav molekulární a translační medicíny Lékařské fakulty Univerzity Palackého v Olomouci  
Hněvotínská 5, 779 00, Olomouc  
Kontaktní osoba: Mgr. Peter Vanek  
mob.: +420 775 050 355, email: peter.vanek@upol.cz

damage response (Fancd2, 53BP1) and senescence (p16Ink4a and p21). To prepare models expressing citrine-tagged versions of protein products of Fancd2 and 53BP1 we targeted directly genes loci of these genes. In p16Ink4a and p21 reporter mice strategy we inserted genes encoding for luciferase and tdTomato under p16Ink4a (or p21) promoter control into ROSA26 locus. Mouse embryonic fibroblasts were developed from created mouse lines and the activity of tagged proteins was examined. Our models could be used for deeper analysis of the role of senescence and DNA damage response in context of cancer development and its treatment.

**Genome editing and gene modification technologies: an overview and update**

úterý / 2. prosince 2014 / 13.30 - 13.45 hod.

**Silvia Petrezselyova, Radislav Sedlacek**

Laboratory of Transgenic Models of Diseases and Czech centre for Phenogenomics, BIOCEV, Institute of Molecular Genetics of the ASCR, v.v.i., Prague, Czech Republic

**Introduction**

Functional gene studies require precise and efficient genome engineering technologies and gene targeting via homologous recombination (HR) has been extensively used to generate specific mutant species for decades. However, the use of this technique has been hampered because of several limitations: low HR rate in mammalian cells, labor-intensive and time-consuming selection/screening strategies and construction of large targeting vectors. In recent years, discovery of new genome-editing technologies, such as ZFN (zinc finger nucleases), TALENs (transcription activator-like effector nucleases) and CRISPR (the Clustered Regularly Interspaced Short Palindromic Repeats) associated with Cas9 (CRISPR-associated 9) protein, has revolutionized

generation of targeted mutations in many model organisms. All these technologies work on the same principle, i.e. sequence-guided DNA endonucleases induce DNA double-strand breaks that subsequently stimulate either non-homologous end joining (NHEJ) recombination and/or homology-directed repair (HDR) system at targeted loci. The NHEJ recombination is an error-prone event forming small insertion or deletion (indels) and therefore results in a frame-shift mutation. Because the HDR system requires a DNA template to repair a DSB, it is used to introduce a desired point mutation or insert a missing gene/reporter gene.

**Materials/methods**

In our laboratory, we employ both TALEN and CRISPR/Cas9 approaches to create site specific modifications in the mouse genome. Knock-out mice are prepared by targeting one site or two sites simultaneously that allows frame-shift and deletion mutations, respectively. Double-stranded constructs or single-stranded oligonucleotide are introduced via HR to generate point mutation changes, reporter genes or conditional alleles. TALEN and CRISPR/Cas9-related constructs are microinjected into mouse zygotes to generate gene knock-out or knock-in mice or transfected into embryonic stem (ES) cells for the creation of recombinant ES cell clones.

**Results and conclusions**

Transgenic and knock-out mice are valuable models for understanding of physiological functions of proteins and their mechanisms. Our model mice will be applied in many human disease studies, including cancer. Several examples (single point mutation mice, simple/conditional knock-outs and reporter mice) out of about 39 finalized and 30 ongoing projects will be presented.

**Understanding biological heterogeneity with the CyTOF 2 Mass Cytometer**

úterý / 2. prosince 2014 /

13.45- 14.00 hod.

**Mark D. Lynch**

Fluidigm Europe BV, Les Ulis, France

**Introduction**

Single-cell biology endeavors to unravel biological heterogeneity using multidimensional approaches. Cells use DNA, RNA, and proteins to power biological networks.

**Materials/methods**

The C1TM Single-Cell Auto Prep System delivers an easy, complete workflow that captures and prepares individual cells for gene expression and sequencing, while the CyTOF® 2 Mass Cytometer allows high-speed acquisition of multiparametric single-cell proteins.

**Results and conclusions**

With these innovative tools, multidimensional single-cell biology is providing profound insights into the dynamic elements of biological heterogeneity.

**Three-dimensional cultures: physiologically-relevant in vitro tumor models**

úterý / 2. prosince 2014 / 14.00 - 14.15 hod.

**Viswanath Das, Marta Zbožínková, Marián Hajdúch**

Institute of Molecular and Translational Medicine, Olomouc, Czech Republic

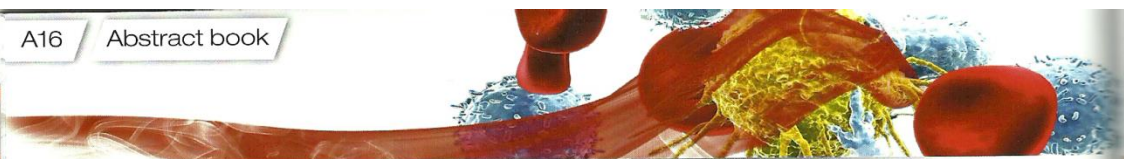
**Introduction**

Three-dimensional (3D) cultures of cancer cells are increasingly being recognized as physiologically-relevant in vitro tumor models for effective selection of anticancer drugs in preclinical studies. Herein, we present a comparative study of the effect of a few selected anticancer agents that are clinically used in the treatment of various solid tumors in two-dimensional (2D) and 3D cultures of colorectal HCT116 and HT29 carcinoma cells.

**Materials/methods**

**Methods**

Cytotoxic effects of anticancer agents in 2D and 3D cultures of



HCT116<sup>+</sup> and HT29 cells were examined using MTT cell proliferation assay and bright-field imaging. Cell cycle alteration in 3D cultures was monitored by flow cytometry. Changes in the expression of proteins in 2D and 3D cultures were detected by Western blot analyses.

#### Results and conclusions

Anticancer drugs that are highly cytotoxic in 2D cultures show low cytotoxicity in 3D cultures of HCT116 and HT29 cells. 3D cultures of HCT116 and HT29 cells showed G0/G1 cell cycle arrest and an increase in the expression of carbonic anhydrase IX. Our results illustrate relative closeness of three-dimensional cultures to primary tumors and provide further support for the potential use of 3D cell cultures for the screening of promising anticancer agents in preclinical screens.

**Výhody vysokokapacitního qPCR pro genové expresní profilování. Analýza a aplikace. (Advantages of high-throughput qPCR for gene expression profiling. Analysis and applications.)**

úterý / 2. prosince 2014 / 14.15 - 14.30 hod.

***Vlasta Korenková<sup>1</sup>, Lucie Langerová<sup>1</sup>, Vendula Novosadová<sup>1</sup>, Mikael Kubista<sup>1,2</sup>***

<sup>1</sup> Biotechnologický ústav AV ČR, v.v.i., Praha, Czech Republic,

<sup>2</sup> TATAA Biocenter, Goteborg, Sweden

#### Introduction

Expresní profilování představuje měření exprese více genů najednou za účelem vytvoření obrazu o buněčné funkci. Profily genové exprese mohou být použity například pro diagnostické monitorování odpovědi pacienta na léčbu a tím k optimalizaci individuální terapie.

#### Materials/methods

Vysokokapacitní zařízení BioMark (Fluidigm), které je umístěno

v qPCR servisním pracovišti Biotechnologického ústavu AV ČR, umožňuje současnou analýzu exprese až 96 genů v 96 vzorcích (9216 reakcí) v rámci jediného experimentu. Měření probíhá pomocí kvantitativní polymerázové řetězové reakce (qPCR), která je jednou z nejcitlivějších metod pro kvantifikaci mRNA či mikroRNA. Možnost analyzovat větší množství genů najednou vybízí k použití multivariálních statistických analýz.

#### Results and conclusions

Využití vysokokapacitního qPCR přístroje BioMark poskytuje množství výhod. 1. Efektivita: Výrazná úspora vzorku (5 µl pro kompletní analýzu), detekční chemie, mastermixu a spotřebního materiálu. 2. Rychlost: Celý vysokokapacitní experiment lze provést v rámci několika hodin, ne dnů či týdnů. 3. Automatizace a vysoká kapacita: Díky zautomatizovanému pracovnímu postupu je minimalizována možnost lidské chyby. Není potřeba mezidestičkové kalibrace. 4. Sensitivita a flexibilita qPCR systému. 5. Možnost dalších aplikací: vysokokapacitní genotypování a digitální PCR.